BUBBLE BARRIER TECHNOLOGIES FOR COMMON CARP

A THESIS
SUBMITTED TO THE FACULTY OF THE GRADUATE SCHOOL
OF THE UNIVERSITY OF MINNESOTA
BY

Daniel Patrick Zielinski

IN PARTIAL FULFILLMENT OF THE REQUIREMENTS
FOR THE DEGREE OF
MASTER OF SCIENCE

Dr. Vaughan Voller, Dr. Miki Hondzo

March 2011

Acknowledgements

I would like to thank the Legislative-Citizen Commission on Minnesota Resources (LCCMR) for providing the funding for this project.

Drs. Vaughan Voller, Miki Hondzo, and Peter Sorensen provided great help through the experimental design and data analysis. Their guidance and technical expertise was invaluable and this research would not have been possible without them. A special thanks to Jon Svendsen for his help in developing the PIT-tag tracking system and carp testing procedure.

The entire St. Anthony Falls Laboratory technical staff provided significant insight for the experimental flume measurements of individual bubble diffusers. Jay Maher was integral to performing all the carp trials at the Aquaculture Center. Brian Moe and Hangkyo Lim also deserve special thanks for performing all the daily care of the carp in St. Paul. The Statistical Consulting Service at the University of Minnesota and in particular Aaron Rendahl helped with the analysis of the carp passage data.

Dedication

This thesis is dedicated to my wife, Amanda, and daughter, Lorelai, for their love and support.

Abstract

Great ecological benefit will be gained if effective barriers can be constructed to control the movement of invasive common carp. Carp feeding habits lead to an over-enrichment of nutrients in lakes that dramatically reduces water quality and ecosystem health. Bajer et al. [2010] demonstrated that in Minnesota lakes, juvenile carp are recruited from nursery lakes to larger water bodies through small connecting channels. Reducing juvenile carp recruitment through the use of a barrier at the entrances to the interconnecting channels could prove useful in an integrated carp management plan for the entire watershed. Current barrier technologies are not well suited for these sites due to the shallow water and rapidly changing water level. This research focuses on the use of bubble curtain barriers, which has been relatively ignored in previous barrier studies, as a barrier technology that shows promise for this application. Bubble curtains generate distinct acoustic and hydrodynamic fields, and through proper manipulation could be used to deter juvenile carp migration.

The initial stage of the barrier design was to quantify and measure the physical fields generated by a bubble curtain. An understanding of the physical fields helps to design full barrier systems by exploiting certain features of the bubble curtains. Experimental data revealed that a coarse-bubble curtain created a weaker flow field, but a stronger acoustic field than a fine-bubble diffuser. The subsequent stage of research included barrier tests with live carp using a PIT tag tracking system, which allowed quantification of carp passage over a barrier sans video recording. Three incrementally stronger bubble barriers were designed. A single diffuser design exhibited a mildly retarding effect of carp passage time (passages were delayed 10-15 sec) but not on the actual number passage attempts. Two separate multi-diffuser barriers (varying in configuration and air-supply) exhibited approximately a 75% decrease in carp passages, in upstream and downstream directions. The reduction of passes for each barrier was calculated by taking the ratio of the number of passages during a barrier-on trial to the number of passages during a control (barrier-off) trial. Carp mobility remained constant between tests, indicating that the two larger barriers did not limit total carp activity, but limited carp passage over the barrier.

This research represents the first stage of characterization of bubble curtain features with respect to carp sensory systems and rigorous testing of bubble barriers under controlled laboratory settings. The experimental results suggest that bubble barriers create a flexible barrier that appears to deter juvenile carp movement in shallow channels, and may prove to be an effective tool in an integrated carp management plan.

Table of Contents

List of Tables

List of Figures

Chapter 1.0 Introduction

1.1 Introduction to Invasive Populations of Common Carp

The common carp (*Cyprinus carpio*) is a highly invasive species in Minnesota Lakes, which may comprise of the majority of the biomass in many lakes [Bajer et al., 2010]. The feeding habits of this species significantly disrupt lake sediments which can lead to an over-enrichment of nutrients that reduce water quality and ecosystem health [Bajer et al., 2009]. Control of carp populations is paramount to reversing the watershed degradation caused by invasive populations. A key to carp population control may be obtained from their life history, which evolved to exploit geographic regions that contain large areas of unstable habitats that can serve as carp nursery lakes [Bajer et al., 2010]. The Upper Mississippi River Basin, in Minnesota, is characterized by networks of interconnected rivers and lakes whose shallow basins frequently experience severe winter hypoxia and fish mortality ("winterkill") [Magnuson et al., 1985]. Winterkill reduces the number of native predators of carp eggs and larvae in the nursery basins, improving the chance of maturation of carp larvae [Bajer et al., 2010].

Bajer et al. [2010] identified two potential nursery basins in Minnesota and correlated recruitment from the nursery basins to larger lakes with hypoxic events. Carp populations within the larger lake were directly related to the recruitment of juvenile carp from the nursery basins after hypoxic conditions. A barrier developed to limit or stop this migration would pose as a useful tool in an integrated carp management plan for the entire watershed. Recruitment of juvenile carp from nursery lakes to the larger lakes requires small interconnecting channels between water bodies, with typical dimensions of

<0.5m deep and 1-3m wide, and provides an ideal constriction for which a barrier would be located. These channels usually experience seasonal flooding, which along with the diminutive size of the channel and shallow water makes most current barrier technologies unattractive. This research focuses on the use of bubble curtain barriers, which has been relatively ignored in previous barrier studies, as a barrier technology that shows promise for this application. Bubble curtains generate distinct acoustic and hydrodynamic fields, and through proper manipulation could be used to deter juvenile carp migration. Besides the physical stimuli generated, a bubble barrier is an attractive option as it does not obstruct flow in the channels. As the use of acoustic and hydrodynamic barriers for the control of invasive species remains largely untested [Webb et al., 2008], the goal of this research was to systematically identify the physical fields generated by a bubble curtain and assess the effectiveness of bubble curtain barrier technologies as a means of controlling juvenile carp movements.

1.2 Alternative Barrier Technologies

A site for a juvenile carp barrier identified in this research has several site constraints that make some current barrier technologies unattractive. Nursery lakes, like those identified by Bajer et al. [2010], are relatively shallow (≈ 1m deep) with outlets approximately 2-3m wide. Often found in wetlands, the nursery lake outlets can be difficult to reach and be a bottleneck for debris and flotsam in the lakes. Any barrier installed should not catch this debris or require frequent maintenance, as a means to reduce operation costs. The remote location also restricts what kind of infrastructure is available to power a barrier.

Finally, the barrier must be flexible to changes in water level and flow to account for seasonal flooding.

Several alternative fish barrier technologies exist, providing stimuli that most fish are able to detect including sound, light, chemical, pressure, and electric currents [Popper et al., 1998]. Table 1 provides a list of alternative barrier technologies and respective advantages and disadvantages for use at a nursery lake outlet. As noted in Taylor et al. [2005] and Welton et al. [2002], there exists proprietary devices that combine multiple stimuli sources. Combination barriers require significant room to fit all the equipment and may be difficult to install in shallow channels.

Based on Table 1, bubble barriers provide a relatively low cost/maintenance barrier that should not obstruct the outflow of the lake in comparison to alternative technologies. Another promising feature is that bubble curtains create multiple sources of stimuli (flow and sound) that could be exploited for juvenile carp deterrence. Lastly, the lack of peer-reviewed literature addressing bubble barrier technology makes it an ideal candidate this research.

Table 1-1
Alternative Barrier Technologies

Barrier Type	Description	Advantages	Disadvantages	Source(s)
Chemical	Plant based chemical, rotenone, applied to invaded water to kill aquatic species since 1940's	Highly effective at known doses; compound readily degrades; not impact on flow	Not species specific; requires repeated application in moving water, high effort to recover affected fish	[Meadows, 1973]
Physical	Any physical structure limiting fish passages (i.e. dams, grated structures)	Impedes all movement in up- and down-stream passage of all fish	Not species specific; strict regulation for dams; high maintenance due to debris	[French et al., 1999]
Visual	Strobe light with set flicker speed in water	Relatively little intrusion into flow; flexible with flow speed; highly effective with bubble curtain on some species	Highly dependent on natural light levels; turbid water reduces effectiveness; not proven on all species	[Patrick et al., 1985; Popper et al., 1998]
Acoustic	Underwater speaker with specified signal	Flexible to flow conditions; potentially species specific; wide range of sound production	Not well represented in peer-reviewed literature; expensive equipment that could catch debris	[Webb et al., 2008; Taylor et al., 2005; Popper et al., 1998]
Bubble	Forced air through diffuser to produce bubble curtain	Flexible to some flow conditions; potentially species specific; broad physical stimuli; relatively simple construction and low cost	Not well represented in peer-reviewed literature; may be "washed out" under high flows	See Section 1.3
Electric	Electric current produced by electrodes located on channel perimeter	Proven highly effective against upstream migrating fish	Expensive equipment and maintenance; health risk to people and animals; not species specific	[Popper et al., 1998]

1.3 Literature Review of Bubble Curtains

Only a few peer-reviewed publications on the use of bubble curtains as a fish barrier exist. These studies focus on a range of species including bighead carp [Taylor et al., 2005], atlantic salmon [Welton et al., 2002], eurasian ruffe [Dawson et al., 2006], and gizzard shad, alewife, and smelt [Patrick et al., 1985]. Taylor et al. [2005] and Welton et al. [2002] studied the use of a bubble curtain in conjunction with an independent sound projector. Bubble diffusers were created by holes drilled into PVC pipe with air flow rates ranging from approximately 0.1 to 1.0 $Ls^{-1}m^{-1}$. The diffuser utilized by Taylor et al. [2005] and Welton et al. [2002] was a proprietary device developed by Fish Guidance Systems. Taylor et al. [2005] experimental results showed that the bubble curtain in conjunction with a sound projector decreased bighead carp passages by 95%. Welton et al. [2002] showed 20-40% efficiency during daylight and >70% efficiency during nighttime of deflecting atlantic salmon smolt. These studies did not focus on using the bubble curtain as a primary means to deter the fish, nor was there an in-depth analysis of the physical fields generated by the barrier. Patrick et al. [1985] indicated that the three species listed avoided an air bubble curtain generated by a single wand of porous plastic pipe, but provided little detail of why it was effective.

Despite the somewhat positive results previously listed, other publications did not show the same promise for bubble barriers. Dawson et al. [2006] studied the effectiveness of a bubble curtain and an electrical barrier, separately. The bubble diffuser utilized consisted of 0.4 to 1.0 mm holes drilled at evenly spaced distances of either 6.25 or 12.5 mm. Instead of deterring eurasian ruffe, a slight attraction to the bubble barrier was observed.

Other sources such as Taft [2000] states that in review of numerous tests in the Great Lakes, air bubble curtains as the sole deterrent for fish has been generally ineffective; however, it was suggested that pairing the bubble curtain with other deterrent technologies (i.e. sound generator, or strobe lights) may be an effective means to deter fish. EPRI [1998] also published a report indicating that common carp, among other fish species, did not display an avoidance response to an air bubble curtain or engineered sound field. Detailed characteristics of the engineered sound field were provided, but no effort was made to quantify the acoustic properties of the bubble curtain. The bubble diffuser used in the EPRI [1998] experiment was constructed of cast iron pipe with 1.5mm diameter holes spaced at 38.1cm over 24.4m of pipe. The air flow rate provided to the barrier was approximately 0.2 $Ls^{-1}m^{-1}$. As is shown in the available literature, bubble curtain barriers have shown mixed results ranging from relatively effective with a sound projector [Taylor et al. 2005;Welton et al. 2006] to not effective at all [EPRI, 1998; Taft, 2000]. A goal of this research is to provide comprehensive analysis of bubble curtain barriers as a deterrent to juvenile carp migration, and provide some explanation why such various results have been published. No peer-reviewed publications could be found that characterize the sound field generated by a forced air bubble curtain as a means to deter fish movement.

Outside of the aquaculture field, bubble curtains or diffusers have been studied by engineers and scientists as a means to aerate and induce mixing in stratified lakes. These studies have investigated the generated velocity fields [Brevik et al., 2002; Fannelop et al., 1991,] and turbulence (Chen et al., 2001); however, the depths considered for these

studies were considerably greater than 1m for most cases. The bubble curtains used in the Brevik et al. [2002] and Fannelop et al. [1991] study were coarse bubble diffusers made by drilling 0.8 to 0.5 mm holes into a steel pipe and plexiglass tube with an air flow rate ranging from approximately 1 to 4.5 $Ls^{-1}m^{-1}$. The acoustic properties of bubble curtains have been exploited for the mitigation of underwater construction noise. Nehls et al. [2007] demonstrated that a bubble curtain attenuates sound through the principles of sound scattering and an individual bubble's resonant frequency. While these studies focus on large scale bubble dynamics, Lin [1994] discussed the controlling factors of individual bubble sizes created by forced air through an orifice and Leighton [1994] provides a comprehensive description on the acoustic properties of individual bubbles. Review of the engineering literature clearly indicates that the hydrodynamic features of bubbles curtains occurs across a wide variety of scales ranging from bubble size (1-10mm) to the bubble plume size (1-10m).

Note that the term "bubble curtain" pertains to a linear bubble plume generated by pressurized air forced through a single diffuser, while a "bubble barrier" refers to any combination of diffusers or type or orientations to create a comprehensive barrier of bubbles.

1.4 Objectives and Scope

The objectives of the ongoing research project were as follows:

1. To identify and quantify the physical fields generated by a bubble curtain, as well as understand of how these fields can be manipulated to deter juvenile carp migration. The physical fields identified are those that can be linked to specific

detections systems of carp. This step will provide insight to what physiologic responses may be expected during live specimen testing.

2. Design and develop a carp barrier that exploits the characterized physical fields and the predicted response to such stimuli.
3. Test the effectiveness of each barrier technology with live specimen. This also includes development of a detection system and testing protocol that can reliably track carp movement in a laboratory flume.

Chapter 2.0 Characterization of Physical Fields

The premise of a bubble barrier design is to create a physical field that is detected by carp and results in an avoidance response. Detailed measurements which characterize the physical fields generated by a bubble curtain will help create a clear link to what physiologic responses may cause carp to be deterred by the barrier. Webb et al. [2008] identified that hydrodynamic and acoustic fields may warrant an avoidance response in fish, and that this area of fish passage control in largely untested. Hydrodynamic fields discussed in this document pertain to fluid flow characteristics such as velocity fluctuations and turbulence generated by bubble curtains. Acoustic fields discussed in this document pertain to pressure wave fluctuations, quantified as sound pressure level (SPL), generated by the bubble curtain. Both fields are detected by two different fish sensory systems, lateral line system and the auditory system (i.e. inner ear). Differences in the nature of the fields allow for a broad spectrum of measurement techniques and analyses to be used in the design of alternative juvenile carp barriers. This section will outline basic carp sensory systems with respect to flow and sound generated by the bubble curtain, laboratory set-up used for physical measurements, individual bubble characteristics, and full scale physical measurements. Physical fields quantified in this section are theoretically considered important to deterring juvenile carp as no behavioral tests were performed that isolated either fields or sensory system.

2.1 Function of the Carp Octavolateralis System

The octavolateralis system is responsible for detection of pressure fluctuations (inner ear), orientation and body motion sensation (vestibular system, also controlled by inner ear), and flow field fluctuations (lateral line system) [Webb et al., 2008]. The main

distinction between the lateral line system and inner ear is that the lateral line detects particle motion while the inner ear detect pressure fluctuations. Both systems also rely on a similar hair cell that performs the same mechanosensory function to detect a physical field [Popper et al., 1998]. The vestibular system is primarily a monitoring system of the fishes own body movements and location, not so much of an active detector for physical fields, so the remaining focus will be on the lateral line system and inner ear.

The lateral line system, present in most fish, is a hydrodynamic receptor system which is split between two subcategories: superficial neuromasts (SN) which are located throughout the skin, and the canal neuromasts (CN) which are located in the lateral line canals. Neuromasts are used to detect minute water movements caused by stimuli such as ocean currents, tides, river flows, wind, and various other large- and small-scale flow structures apparent in aquatic environments [Webb et al., 2008]. Each neuromast has a similar structure to the maculae found in the inner ear of fishes, and consists of a bundle of sensory hair cells as seen in Figure 2-1.

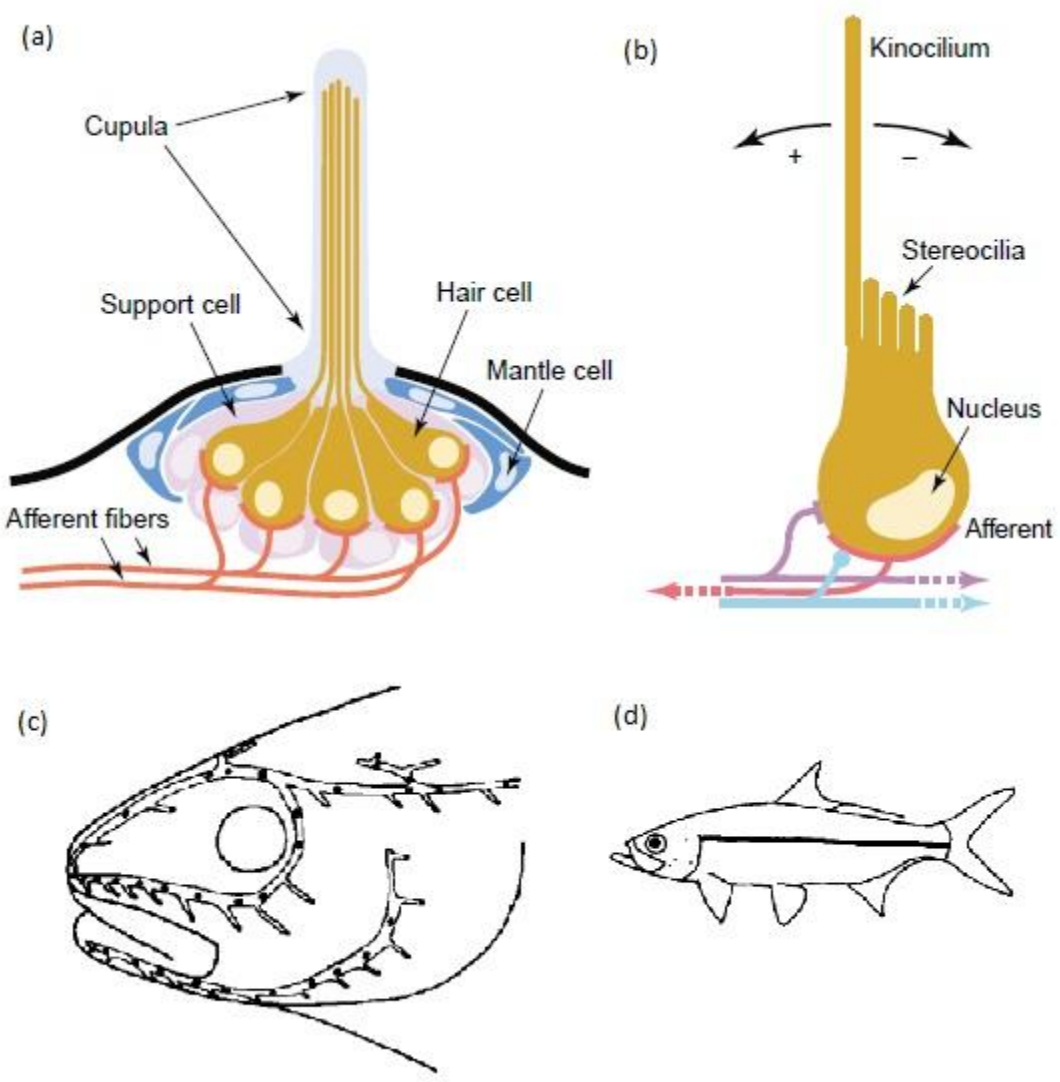

Figure 2-1. (a) and (b) Display the typical superficial neuromast composition [Ghysen et al., 2004]; (c) dark spots represent the typical location of superficial neuromasts on the head [Webb et al., 2008]; (d) the line represents the typical location of the lateral line [Webb et al., 2008]

Shearing of the hair cells by fluid movement, with displacements of as low as 1 nm, causes a neural response; however, displacements greater than 100 nm can cause an oversaturation [Webb et al., 2008] and prevent any further fluid movement detection. An oversaturation of fluid motion does not necessarily lead to an avoidance response. Neuromasts range in size from 10 to 400μm in length and can detect minute fluid

motions, hypothetically small eddies, along with the mean fluid flow [Webb et. al., 2008]. The particle motion associated with a pressure wave may also be detected by the lateral line system; however, particle motion related to a pressure wave is only substantial enough for detection in the very-near field (two to three body lengths) [Popper et al., 1998]. Lateral line sensitivity in carp is not substantially different than most native species. Therefore, if fluid flow is determined to be the primary cause of deterrent, native species are just as likely to be effected as carp.

The primary sensory organ responsible for detecting sound pressure stimuli in fish is the inner ear. The fish inner ear is generally comprised of three semicircular canals (detect accelerations associated with the vestibular system) and three otolith organs (primary sound detection system). The otolith organs contain both an epithelium covered in thousands of sensory hair cells, maculae, and denser otoliths [Webb et al., 2008]. Fish have a similar density to water; therefore pressure waves transmit through fish with relatively little interference. Detection of the pressure wave occurs when the denser otolith moves at a different amplitude and phase as the less dense epithelium, stimulating the maculae [Popper et al., 1998].

Fish are generally categorized as either hearing "generalists" or "specialists". Carp are considered hearing "specialists" because they have specialized rib bones called Weberian Ossicles that allow the swim bladder to act as an additional sound pressure transducer to accompany their inner ear, increasing their sensitivity to sound levels in their environment [Webb et. al., 2008]. Popper et al. [1972] investigated the sensitivity of carp

hearing using pure tones and behavioral response, while Kojima et al. [2005] more recently investigated the sensitivity using neural activity. These independent tests correlated a range sounds with observed behavioral response or specific neural activity to find the minimum amplitude at which a carp can hear a sound at a given frequency. The result of these studies generates the audiogram for common carp provided in Figure 2-2. The advantage of the neural activity measurements [Kojima et al., 2005] is the isolation of inner ear detection from lateral line detection. As is present in Figure 2-2, the hearing range provided by neural activity only is much higher than the behavioral response curve. This difference is accredited to very-near field detections by the lateral line system. Note that the carp's most sensitive region of hearing using is between 100-500 Hz down to a SPL of 60-90 dB (re 1 µPa) {all remaining SPL measurements will be quantified in decibels with reference to 1 µPa).

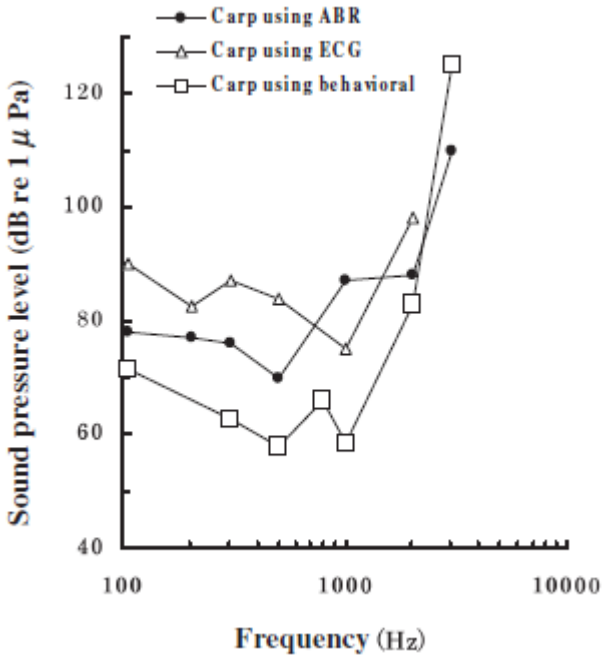

Figure 2-2. Audiogram for common carp using auditory brainstem response (ABR), electrocardiogram (ECG), and behavioral response [Kojima et al., 2005]

Hearing “generalists” usually detects sounds within a range of 50 to 1,500 Hz, but as seen in Figure 2-2 a carp is capable of detecting sounds up to 4,000 Hz. Most native fish to Minnesota are considered hearing “generalists”. An acoustic barrier (sound generated by a bubble barrier) may influence carp more than native fish, potentially making the barrier species specific and much more favorable than most current barrier technologies. This hypothesis will later drive the design of alternative barriers, each increasing the SPL over previous versions.

An important consideration when focusing on acoustic field interaction with fish is the “cocktail party” effect. This effect describes when fish are unable to decipher a specific sound within their hearing range unless it is 10 dB above background levels [Popper et. al., 1998]. Therefore it is critical to control the frequency and amplitude of the sound generated by any barrier so that it is within the carp’s most sensitive hearing range while minimally 10 dB above background levels.

2.2 Laboratory Setup - SAFL

Bubble diffusers were tested at the University of Minnesota’s Saint Anthony Falls Laboratory (SAFL). All testing at SAFL was sans live specimens, as the main focus was to identify and quantify the physical fields regardless of effect on carp. The flume utilized at SAFL was a straight flume, fed by water diverted from the Mississippi River, with the following dimensions: 20 in. wide x 36 in. high x 30 ft long. The bubble diffusers were placed at the mid-point of the flume anchored with a wood base buried in sand. A schematic of the bubble diffuser setup in the flume is provided in Figure 2-3.

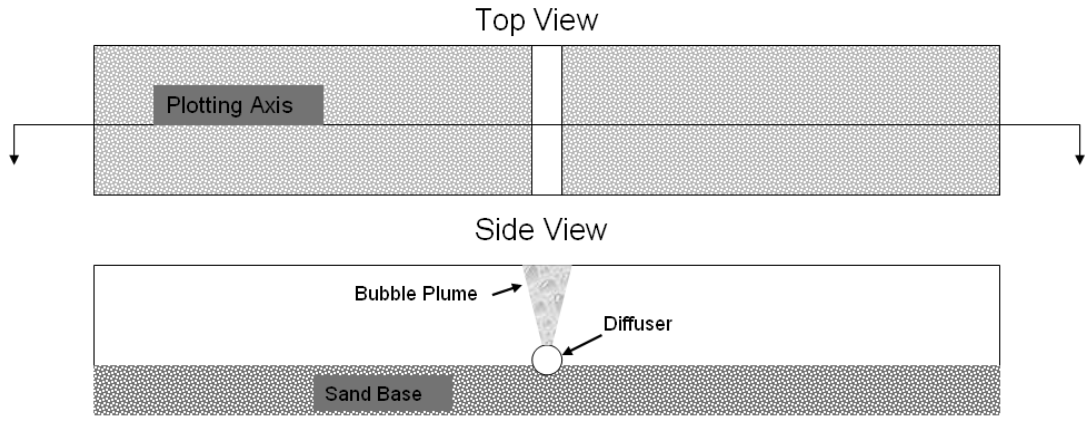

Figure 2-3. Diffuser set-up and measurement location

Air was supplied to the bubble diffusers through a laboratory compressed air line capable of high pressure and high volume. The air supply is monitored and controlled through the use of a pressure gauge and rotameter. Physical fields generated by the bubble barriers are measured by the following list of apparatus along with the specific fields measured:

1. SonTek 16-MHz MicroADV (Acoustic Doppler Velocimeter) – three-dimensional velocity measurements at a sample rate of 50-Hz
2. MSCTI SN 5 (20 K Temperature Probe) – instantaneous temperature at a sampling rate of 100-Hz
3. Dissolved Oxygen Probe – dissolved oxygen level sampled at a rate of 100-Hz
4. BK 8103 Hydrophone – piezoelectric transducer to measure sound pressure level at 50-kHz

Each of these instruments were attached to a mobile cart and mounted on a telescoping arm to repeatedly take simultaneous measurements upstream and downstream of the barriers. As seen in Figure 2-3, all measurements were taken along plane through the centerline of the flume. Velocity measurements from the ADV were collected and analyzed using the SonTek software package HorizonADV and WinADV. The temperature and dissolved oxygen probe data were

collected using a data acquisition board and software program TracerDAQ. A one minute continuous sample was taken at each measurement location of the velocity, temperature, and dissolved oxygen level. Hydrophone data collection required the use of a 5V power pre-amplifier and National Instruments SC-2345 signal conditioning and connector box to digitize the signal. The data was finally collected by the National Instruments software package LabView and further analyzed using Matlab. At each measurement location, four 10-sec sound wave samples were obtained. Temperature and dissolved oxygen levels were measured to gain understanding of fluid interaction with the bubble curtain. No distinct features were evident in these fields to possibly deter carp, therefore the data is not presented in this research.

2.3 Bubble Physical Characteristics

Understanding the formation of a single bubble through an orifice is vital to developing diffusers that can create well defined and predictable physical fields. Bubble formation is driven by two main components, buoyancy and surface tension. The buoyancy force acts to drive the bubble towards the surface, while the surface tension acts to keep the bubble attached around the orifice. As the bubble size increases, the buoyancy force overcomes the surface tension and the bubble detaches from the surface. Bubble formation creates pressure waves (sound) throughout the liquid and accounts for most of the sound generated by a bubble curtain. As the bubbles rise, they coalesce (merge to form larger bubbles). The thickness of the bubble curtain also increases as the bubbles rise. These characteristics were utilized to design two diffuser types; fine-bubble and coarse-bubble.

When a bubble is disturbed by a pressure wave, it causes the bubble wall to pulsate or oscillate at a resonant frequency. Theoretical relationships have been developed to predict the resonant frequency and amplitude of the pressure wave created by an oscillating bubble. Understanding the small scale characteristics of bubbles may provide insight to interpreting the sound signal generated by a bubble barrier, and potentially improve the barrier design. The resonant angular frequency, natural frequency of bubble wall oscillations, of a singular bubble is provided by Minneart's frequency [Leighton 1994]:

$$\omega_o = \frac{1}{R_o}\sqrt{\frac{3\kappa p_\infty}{\rho_f}} \qquad (2\text{-}1)$$

Where

R_o = bubble radius

κ = polytropic index, for air 1.402

p_∞ = pressure in the fluid

ρ_f = density of the fluid

Note that with bubble radius in the denominator, as the bubble size increases, the resonant frequency decreases. The polytropic index characterizes the expansion or compression or gases, in this case air. The amplitude of the pressure wave generated by the oscillating bubble at any distance *r* away from the bubble, assuming no damping, is given by [Leighton et al., 1987]:

$$P_o(r,t) = \frac{A_o(t)\omega_o^2 \rho_f R_o}{\sqrt{\left(1+(kr)^2\right)}} \qquad (2\text{-}2)$$

Where

A_o = amplitude of bubble oscillations

r = distance away from bubble

k = wave number associated with the resonant frequency, given by $\frac{\omega_o}{c}$

c = speed of sound in water ~1480 m/s

The amplitude of bubble oscillations is not easily quantified as this value is typically much less than the radius of the bubble which is on the order of 2-10 mm. High speed photography can be used to estimate the amplitude of oscillations, or back calculated from equation (2-2) using the measured pressure signal. Equation (2-2) does indicate that a larger bubble will generate a greater pressure than a smaller bubble assuming the oscillation amplitude scales with the bubble radius. The relationship in equation (2-1) and (2-2) were used to help characterize the acoustic field produced by each bubble diffuser and help interpret the acoustic data measured.

2.3.1 Coarse-Bubble Diffuser

The first of two diffuser types is identified by the relative large size of bubbles produced when air is forced through the diffuser. Coarse-bubble diffusers consisted of PVC pipe with holes manually drilled at constant spacing. The hole sizes range between 1 mm to 10 mm, and the spacing varies between 0.5 cm to 10 cm. The minimum hole size is determined by the smallest available drill bit and large diameter holes (>10 mm) will not be considered as maintaining a constant air-flow through every hole would be suspect. Figure 2-4 displays the typical bubble curtain generated by the coarse-bubble diffuser. Note the mixture of large and small bubbles.

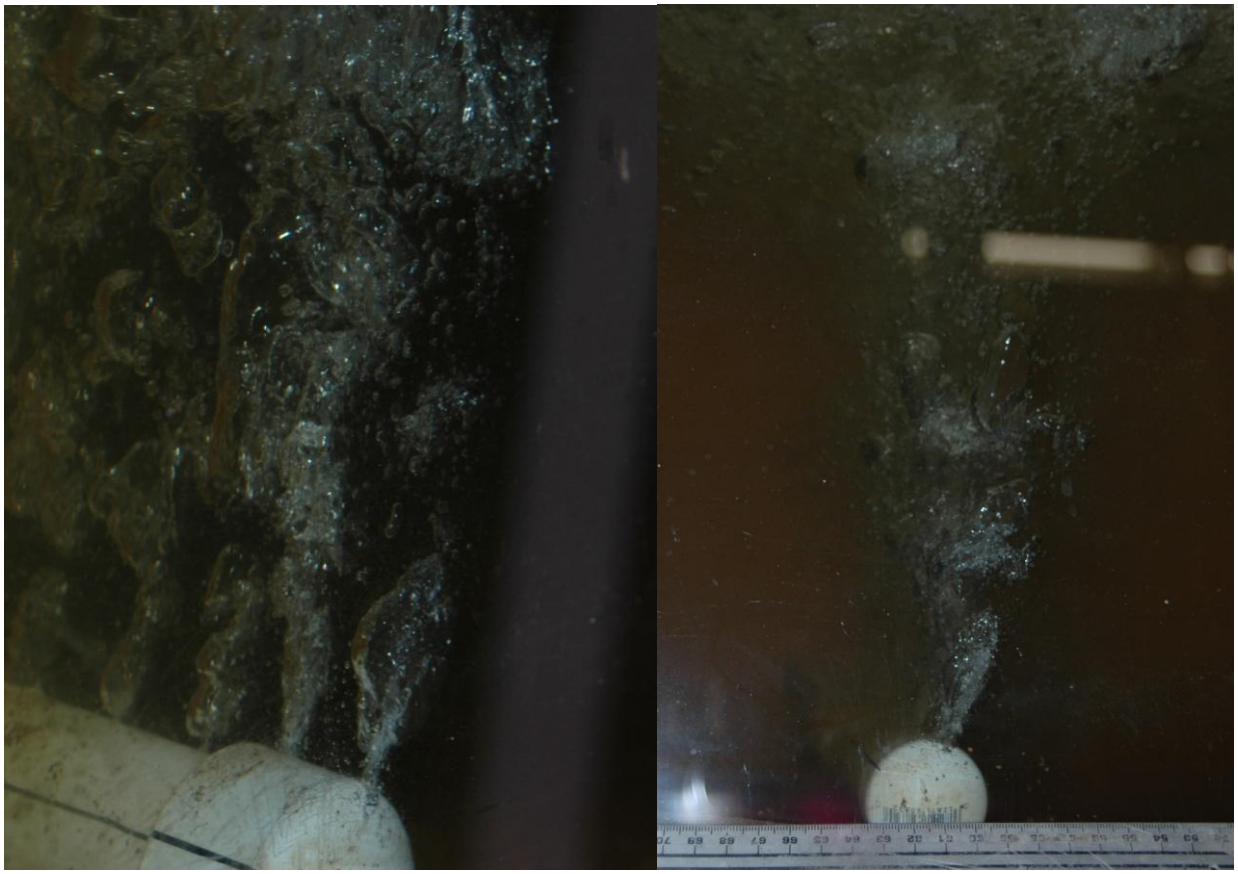

Figure 2-4. Typical bubble curtain provided by coarse-bubble diffuser (1mm holes at 2.5 cm spacing)

Work by Lin et al. [1994] indicated that the diameter of a detached bubble from an orifice will always be larger than the orifice; he also stated that for small orifices, the bubble size in highly dependant on the liquid and diffuser surface tension. The result of this research indicates that 2.5 mm and 1 mm diameter orifices, drilled in the same material, would create similar sized bubbles. As is shown in Figure 2-5, the typical bubble size generated by 1 mm holes near the PVC and surface are approximately 10 mm and 15 mm, respectively. Note the distinct change in shape between the two locations, the bubbles near the PVC are far more elongated (can also be seen in Figure 2-4).

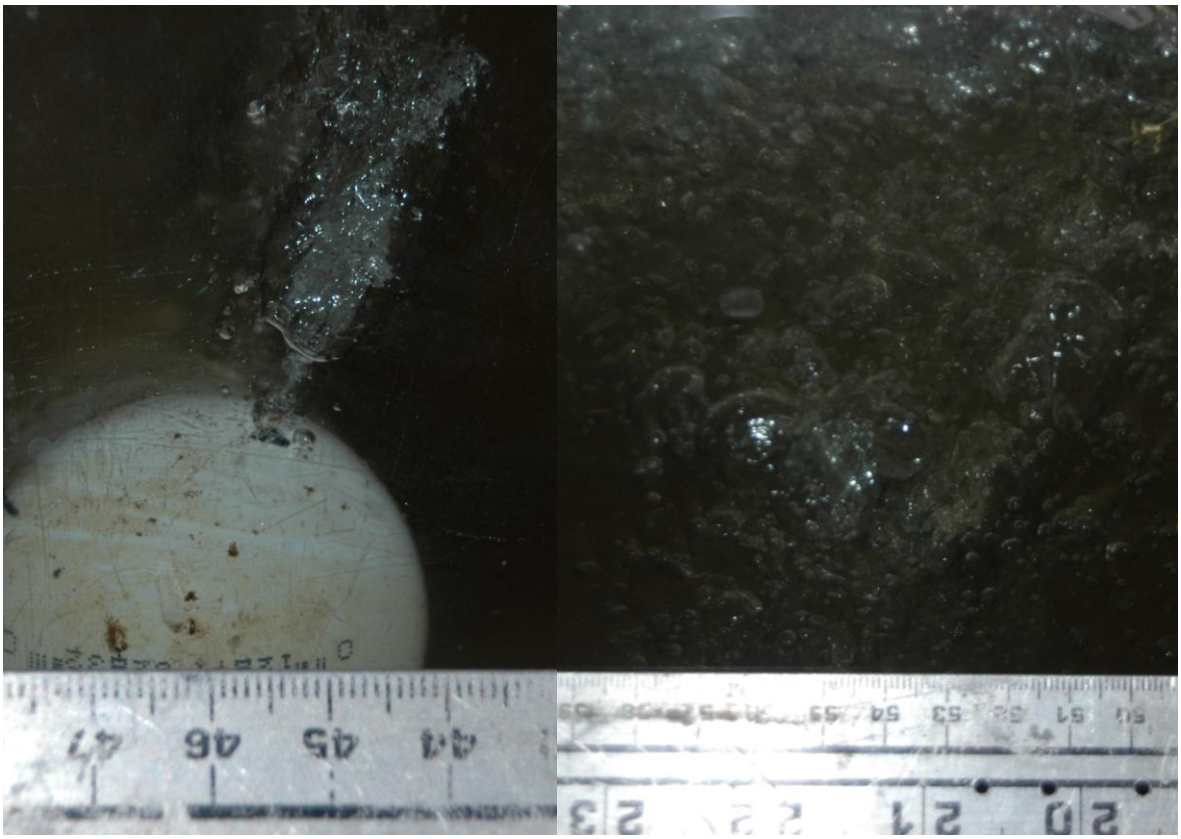

Figure 2-5. Typical bubble size near PVC and at surface for 1 mm holes

The lateral spacing of the holes in the PVC provides control over the density of the bubble curtain. Spacing too large would create gaps near the diffuser, possibly large enough for fish passage. Spacing too small creates immediate overlapping of individual bubble plumes; however, spacing of less than 0.5 cm is time consuming and difficult to maintain a perfectly straight line of holes. Only one line of holes restricts the thickness of the bubble curtain; however, multiple diffusers can be used in series to create a thicker curtain.

The final physical feature that can be controlled to manipulate the bubble curtain is the air flow rate. The PVC pipe used for this application is not rated for high pressures, which limits the maximum air flow rate that can be used. Lin et al. [1994] found that increasing the air flow rate

does not increase bubble size, but increases the frequency at which bubbles are created. As an initial condition for testing, the diffusers will be supplied with a low and high air flow rate of 2.5 and 2.8 $Ls^{-1}m^{-1}$, respectively (flow rates are associated with air pressures of 50kPa and 100kPa, respectively). By inspection, an air flow rate less than 2.5 $Ls^{-1}m^{-1}$ creates a thin, insubstantial bubble curtain. Equation (2-1) theoretically predicts that the coarse-bubble diffuser is capable of generating bubbles with a resonant frequency of 215-320 Hz.

2.3.2 Fine-Bubble Diffuser

The second type of diffuser to be considered for this research is a fine-bubble diffuser, which creates bubbles significantly smaller than the coarse-bubble diffuser. The fine-bubble diffuser consists of porous polyethylene, which is manufactured to have a complex, homogenous pore structure throughout the entire wall. A sample portion of I inch diameter porous pipe with a typical pore size of 35 microns was provided by GenPore Inc. The pore size can be reduced to 10 microns, but with reduced pore size, the chance of clogging increases. The porous pipe is also available in hydrophilic and hydrophobic formulations. The hydrophobic formulation will be utilized in this research based on the work by Lin et al. [1994]. Figure 2-6 displays the typical bubble curtain generated by the fine-bubble diffuser. Note the almost homogenous, dense bubble curtain.

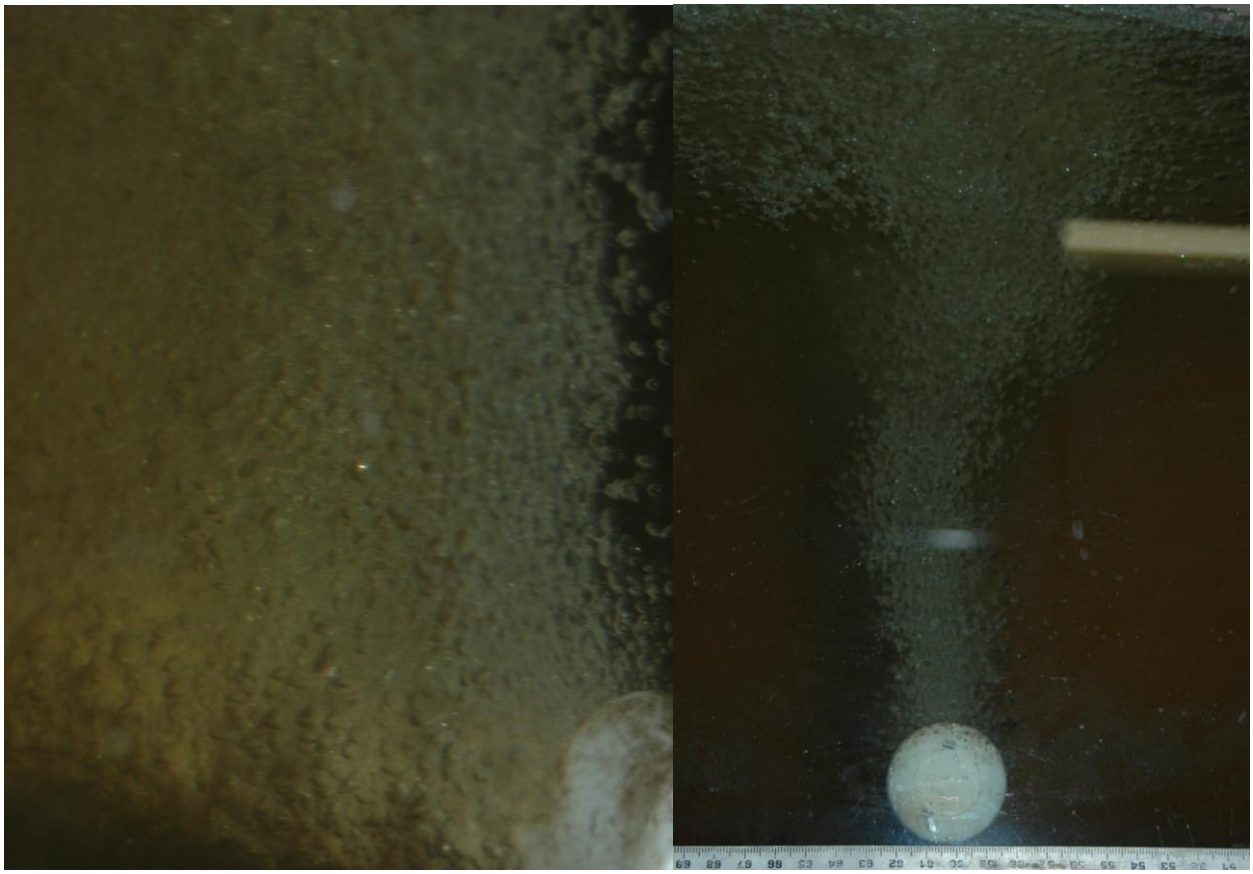

Figure 2-6. Typical bubble curtain provided by fine-bubble diffuser (35 micron holes)

Figure 2-7 displays the typical bubble size near the diffuser and at the surface. Note the homogeneity of the bubble curtain near the pipe and surface in comparison to Figure 2-4 and Figure 2-5.

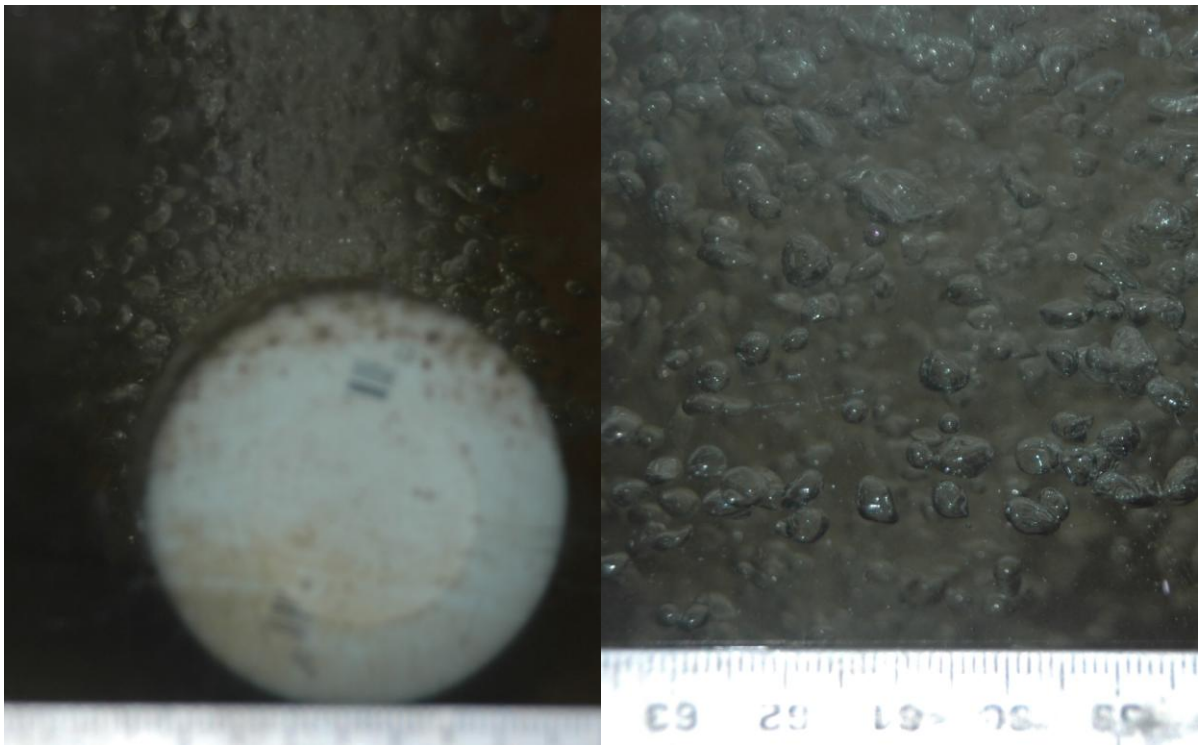

Figure 2-7. Typical bubble size generated by fine-bubble diffuser (35 micron holes)

The typical bubble size is 1-2 mm near the pipe, which is an order of magnitude smaller than the coarse-bubble diffuser formed bubbles. The bubbles near the surface are approximately 2-5 mm in size.

The thickness of the bubble curtain expressed by the porous pipe is slightly thinner than the pipe diameter, as bubbles are formed along the entire surface of the pipe; therefore, the curtain thickness is significantly larger than the coarse-bubble diffuser. Additional thickness of the curtain at bubble formation causes the curtain width near the surface to be thicker than that generated by the coarse-bubble diffuser. The homogenous distribution of pores removes the chance for gaps to form laterally along the diffuser. In general, the bubble curtain created by the fine-bubble diffuser is far denser than that formed by the coarse-bubble curtain for a constant air

flow rate. The fine-bubble diffusers will be subjected to the same air flow rates as the coarse-bubble diffusers. Equation (2-1) theoretically predicts that the fine-bubble diffuser is capable of generating bubbles with a resonant frequency of approximately 3000 Hz.

2.4 Hydrodynamic Fields and Measurements

The measurements taken on flume experiments at SAFL focused on two main physical fields: flow and sound pressure level (SPL). Each diffuser type (coarse-bubble and fine-bubble) was tested individually at two increasing air flow-rates to determine the distinct differences between types, and how the physical fields are manipulated.

2.4.1 Flow Field

The flow field is of interest as water movement intuitively effects fish behavior. The flow field characteristics range from domain scale velocity field, characterized by recirculation cells [Brevik et al., 2002;Fannelop et al., 1991;Riess et al., 1998], to small scale turbulence [Chen et al., 2001;Kundu, 1990]. Characterizing the fluid motion and how diffuser type effects the magnitude of large and small scale fluid motion will help determine which scale of fluid motion influences carp movement more or at all.

Research by Brevik [2002] and Fannelop [1991] have shown that the domain scale velocity field generated by a bubble curtain can be broken down into two subcategories: near- and far-field. The far-field flow is dominated by a horizontal recirculation cell extending approximately two times the depth away from the curtain. The near-field flow is dominated by the vertical velocity of the bubble plume and occurs within close

proximity of the bubbles. The difference between these two categories is the maximum velocity in the far-field acts parallel to the channel flow while the near-field acts perpendicular to the channel flow, creating a sharp velocity gradient. As a carp presumably swims from far- to near-fields, the velocity gradient should be detected and may disrupt an up- or down-stream migration.

The time-averaged velocity vector was calculated at various locations along the centerline of the SAFL flume up- and down-stream of the diffuser, using the MicroADV. The average velocity vectors were obtained to quantify the general flow conditions generated by a bubble plume. From the velocity vectors, the streamlines (the line tangent to the local velocity vector) were calculated for each given diffuser set-up. Figure 2-8 provides the velocity vector plot for the fine-bubble diffuser at an air flow rate of 2.5 $Ls^{-1}m^{-1}$ and set at a depth of 0.25 m. Figure 2-9 provides the corresponding streamline plot to the velocity vectors plotted in Figure 2-8. The streamline plot is included to highlight the location of the stagnation point, or center of rotation of the recirculation cell and location of zero horizontal and vertical velocity. Note the x- and y-axis have been normalized by the depth of flow, resulting in unit dimensions y/D and x/D. Where x and y are the horizontal and vertical directions, and D is the depth of water.

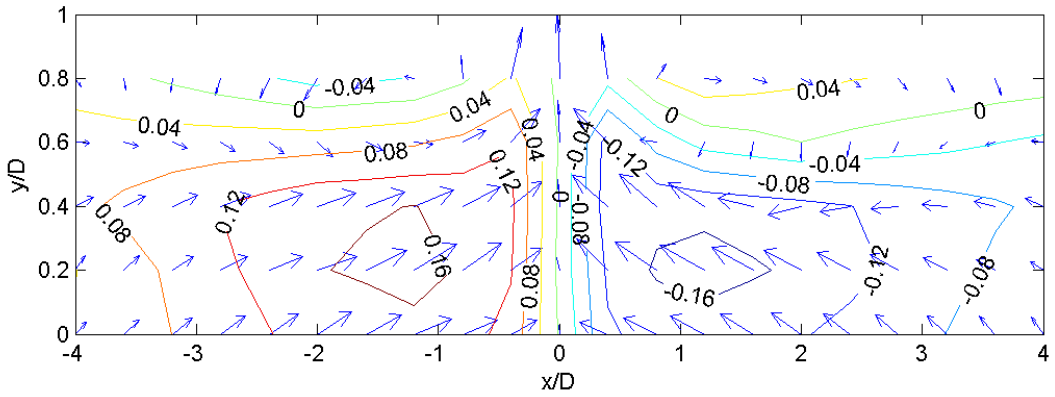

Figure 2-8. Velocity field for fine-bubble diffuser at 2.5 $Ls^{-1}m^{-1}$ and a depth D=25cm (velocity contours are in m/s)

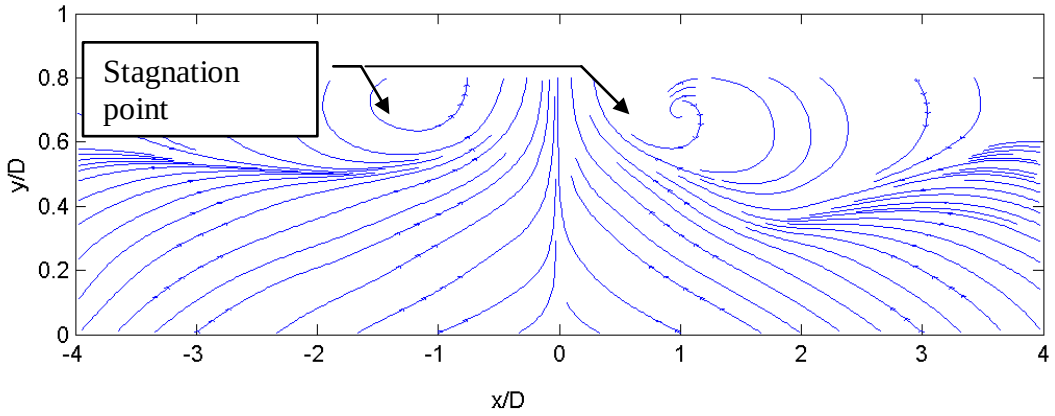

Figure 2-9. Streamline plot of velocity field generated by fine-bubble diffuser at 2.5 $Ls^{-1}m^{-1}$ and a depth D=25cm

Figure 2-10 provides the velocity vector plot for the coarse-bubble diffuser at 2.5 $Ls^{-1}m^{-1}$ and set at a depth of 0.25 m. Figure 2-11 provides the corresponding streamline plot to the velocity vectors plotted in Figure 2-10.

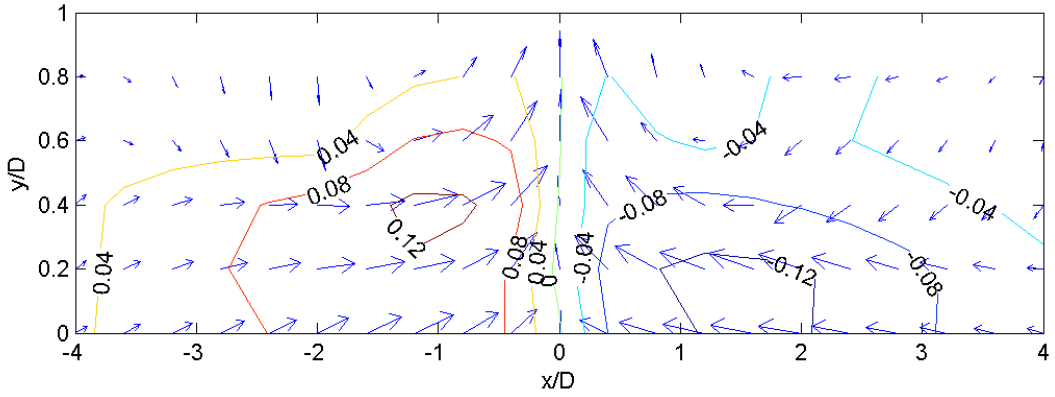

Figure 2-10. Velocity field for coarse-bubble diffuser at 2.5 $Ls^{-1}m^{-1}$ and a depth D=25cm

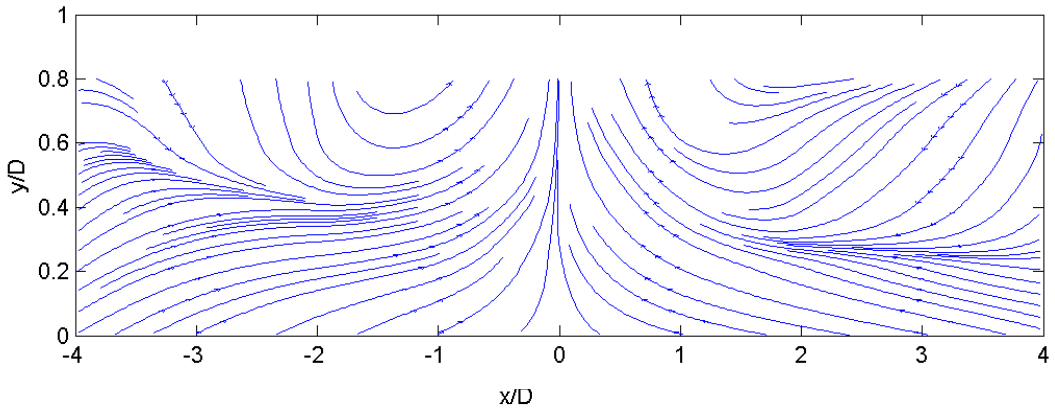

Figure 2-11. Streamline plot of coarse-bubble diffuser at 2.5 $Ls^{-1}m^{-1}$ and a depth D=25cm

Comparison of the two different types of diffusers in Figures 2-8 through 2-11 indicate that the flow generated by the fine-bubble diffuser is stronger than the coarse-bubble diffuser (16 cm/s vs. 12 cm/s). The stagnation point for both configurations is located approximately at a similar horizontal position (x/D = +/-1). The vertical location of the stagnation point with the coarse-bubble diffuser is unknown as it is located shallower than the ADV could measure, while the vertical position is approximately y/D=0.75 for the fine-bubble diffuser. Velocity vectors in Figure 2-9 and 2-11 change from primarily horizontal flow to vertical flow at $x/D \leq 0.5$ away from the bubble curtain, indicating a strong velocity gradient.

Considerable research has been dedicated towards modeling the flow fields generated by bubble plumes; one empirical method used to compare to our data is the entrainment method. The entrainment method relies on the assumption that the "mean flow across the edge of the plume is proportional to […] the mean centerline velocity" [Brevik et al., 2002], or the far-field flow characteristics are dependent on the mean vertical velocity of the bubble plume. The entrainment method developed for line source bubble plumes in a finite reservoir does not utilize a true entrainment assumption, but is based on the similarity to turbulent jet theory. Riess et al. [1998] described the horizontal velocity component of the far-field flow using the following empirical relationship:

$$u(x,z) = \frac{m}{\sqrt{x}} e^{\left(\frac{-z}{kx}\right)^2} - \frac{km\sqrt{\pi x}}{2D} erf\left(\frac{D}{kx}\right) \qquad (2\text{-}3)$$

Where

m = momentum coefficient, fit to data

k = spreading coefficient, fit to data

D = depth of reservoir

Note that m and k are calculated by using least square fits to the measured data. Equation (2-3) assumes the horizontal component of the return flow (towards the plume) follows a Gaussian profile, while the counter flow (away from plume) exhibits a uniform profile. This method is unable to predict velocity field without physical measurements; however, limited surface

velocity is adequate for fitting the momentum and spreading coefficients. Riess et al. [1998] also observed from experiments that the range of influence (length of re-circulation cell) for line source bubble plumes to be between two and seven times the depth. Brevik et al. [2002] developed a similar method assuming both the return flow and counter flow velocity profiles are Gaussian, based on experimental trials. This non-uniform method explicitly calculates the stagnation line (horizontal velocity is zero) away from the vertical bubble plume by the following:

$$\frac{h(x)}{D} = \begin{cases} 0.125(1 + x/D), & x \le 3D \\ 0.5, & x > 3D \end{cases} \qquad (2\text{-}4)$$

Where

h = the depth of the out flowing layer

The horizontal velocity components U_1 and U_2, above and below the stagnation line, respectively, for $x \le 3D$ are described by:

$$U_1(x,z) = u_o e^{\left(-\frac{2z^2}{h(x)^2}\right)} \qquad (2\text{-}5)$$

$$U_2(x,z) = \frac{-u_o h(x)}{D - h(x)} e^{\left[-2\left(\frac{1-z/D}{1-h(x)/D}\right)^2\right]} \qquad (2\text{-}6)$$

For $x > 3D$ the horizontal velocity components are described by:

$$U_1(x,z) = u_o e^{\left(-\frac{8z^2}{D^2}\right)} \qquad (2\text{-}7)$$

$$U_2(x,z) = -u_o e^{\left[-8\left(1-\frac{z}{D}\right)^2\right]} \qquad (2\text{-}8)$$

Where

u_o = the maximum horizontal surface velocity

Experimentally, Brevik et al. [2002] showed that the maximum horizontal surface velocity can be expressed as a function of air flow rate in the following equation:

$$u_o = 1.7\left(gQ^o\right)^{1/3}\left(\frac{P}{D+P}\right)^{1/3} \qquad (2\text{-}9)$$

Where

g = gravitational constant (9.81 m/s^2)

Q^o = unit flow rate of air in diffuser

P = atmospheric pressure as a head of water

The advantage of the method derived by Brevik et al. [2002] is that no momentum or spreading coefficients need to be fit to the data, only the strength of the out flowing jet, which can be calculated using (2-9). The vertical velocity component can be readily derived from the continuity equation. The expression for the vertical component is more complex and of less significance in the far-field; therefore it is omitted.

The empirical methods may provide a useful tool in predicting the range of influence (distance away from plume that flow is influenced by vertical bubble curtain) of a given diffuser design, while also specifying what air flow rate is required to create a recirculation cell that can overcome the mean channel flow (i.e. so the mean channel flow does not sweep the recirculation cell downstream). Figure 2-12 displays the horizontal velocity component measured and predicted by the two models along the depth of the channel at specific locations away from the diffuser. Note that the correlation between the measured and predicted velocities diminishes at distances greater than x/D=2.0. Figure 2-12 clearly shows that the empirical method developed by Brevik et al. [2002] fits the measured velocity relatively well up to two times the depth away from the diffuser.

Fluid motion detected by the lateral line system is not limited to large scale motion of water, as demonstrated by the recirculation cells in Figure 2-8 through 2-11, but includes the small scale water motions that are closer to the scale of a neuromast. First, we must determine if the fluid motion, or eddy, itself is large enough to be detected by a neuromast, yet small enough as to not be interpreted as the mean flow. The first step to validate this hypothesis is to calculate the size of the smallest eddies present in the flow. The smallest scale that an eddy can exist before viscous forces convert the mechanical energy into thermal energy is called the Kolmogorov length scale [Kundu, 1990]. The Kolmogorov length scale was calculated at various points along the centerline of the flume by performing a Fourier transform and cross correlation of the instantaneous velocity data obtained by the MircoADV consistent with [Brigham, 1974;Kundu, 1990;Ramirez, 1985]. Figure 2-13 and 2-14 provide a plot of the Kolmogorov length scale for the fine- and coarse-bubble diffusers in a 25 cm deep flow at an air flow rate of 2.5 $Ls^{-1}m^{-1}$.

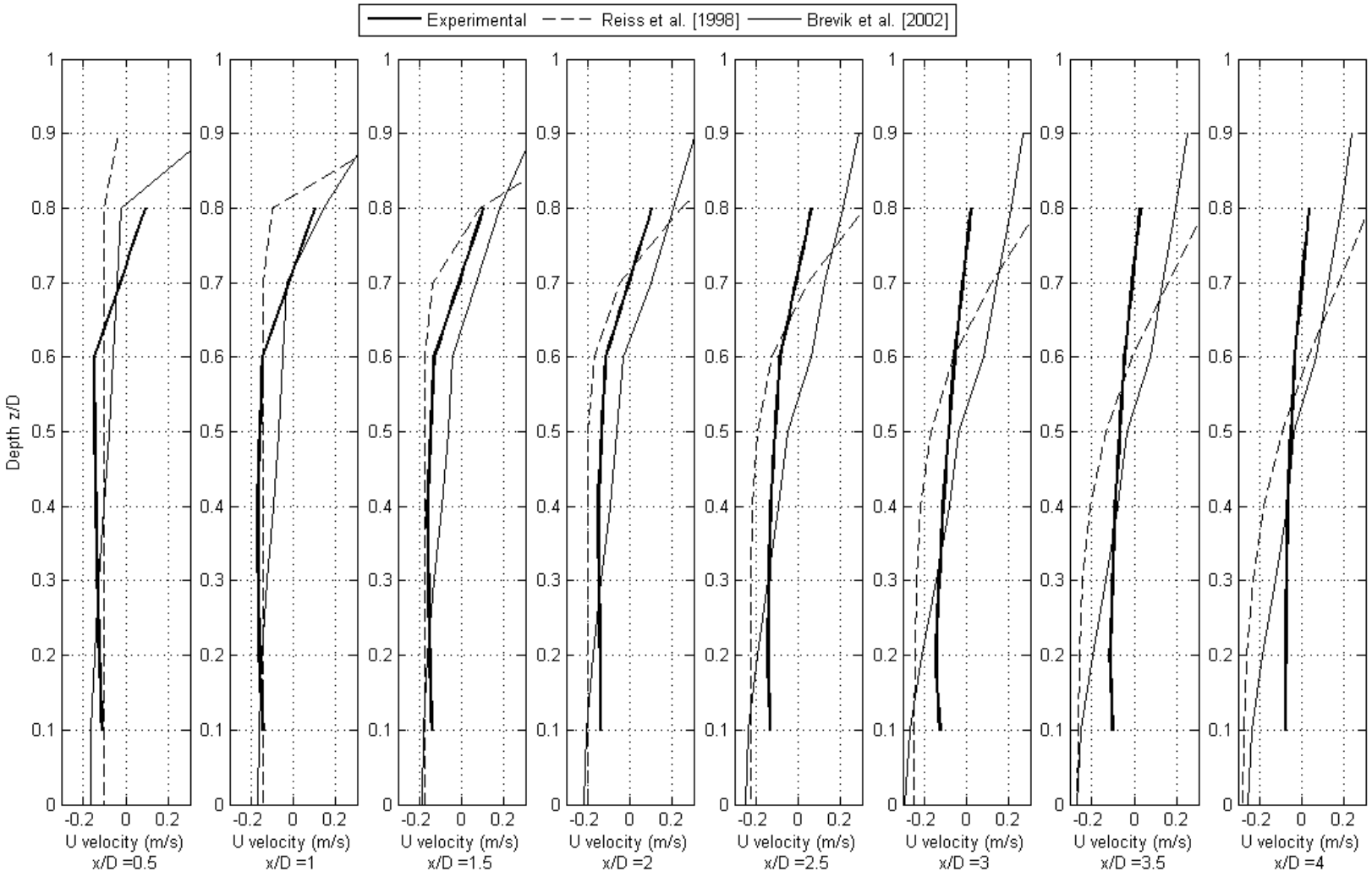

Figure 2-12. The horizontal velocity component of the fine bubble diffuser at 2.5 $Ls^{-1}m^{-1}$ at a depth of 50 cm

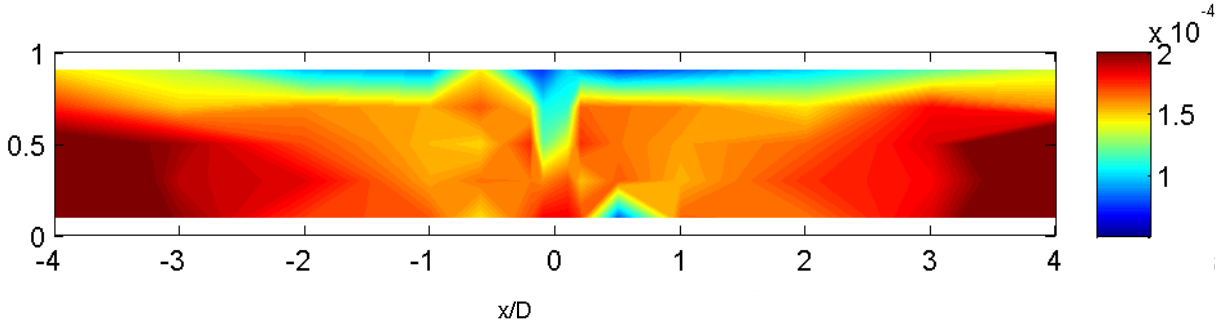

Figure 2-13. Kolmogorov scale for fine-bubble diffuser in depth D=25 cm (scale is in m)

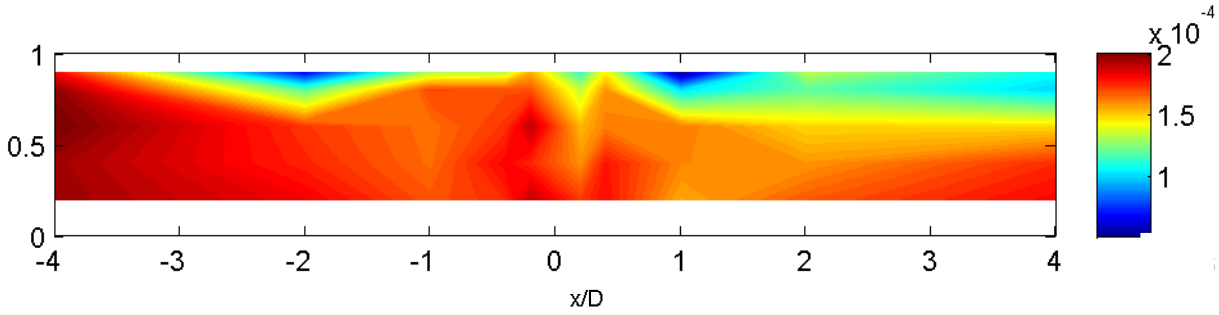

Figure 2-14. Kolmogorov scale for coarse-bubble diffuser in depth D=25 cm (scale is in m)

Note that the eddies are sustained at much smaller scales close to the bubbles and surface, and that there was no significant difference between the fine- and coarse-bubble diffusers. The Kolmogorov length scale of each diffuser is approximately 0.05 mm, which was on the order of the smallest neuromast, and presumably detected by the carp.

The key aspects of each flow measurement including maximum velocity, stagnation point location, and Kolmogorov length scale for each test is included in Table 2-1. The fine-bubble diffuser was tested at a restricted flow rate of 1 $Ls^{-1}m^{-1}$ to match with initial diffuser test with carp at the Aquaculture Center. The fine-bubble diffuser was also tested at 50 cm to see the

effect of water depth on the physical fields. Note that the Kolmogorov length scale does not vary significantly between diffusers; however, the large scale velocity fields are slightly stronger using the fine-bubble diffuser.

Table 2-1
Flow field characteristics of diffusers

Diffuser Type	Flow-rate ($Ls^{-1}m^{-1}$)	Depth (cm)	Maximum Velocity (cm/s)	Stagnation Point Location (X,Y)	Kolmogorov Scale (mm)
Fine-Bubble	1	25	8	(+/-1,0.6)	0.08
	2.5	25	16	(+/-1,0.75)	0.05
	2.8	25	17	(+/-0.8,0.6)	0.06
	2.5	50	13	(+/-1.5,0.75)	0.07
	2.8	50	16	(+/-2,0.75)	0.05
Coarse-Bubble	2.5	25	12	(+/-1,>0.8)	0.05
	2.8	25	13	(+/-1.5,>0.8)	0.04

2.4.2 Sound Pressure Level

The other physical field generated by a bubble plume that was quantified is the acoustic field. As stated earlier, carp are considered hearing specialists because they have specialized rib bones called Weberian Ossicles that allow the swim bladder to act as an additional sound pressure transducer to accompany their inner ear, increasing their sensitivity to sound levels in their environment [Webb et. al., 2008]. Exploitation of this has lead to the development of acoustic barriers to limit movement of carp [Popper et. al., 1998;Taylor et. al., 2005;Welton et. al., 2002].

The limited barrier designs highlighted in literature rely on an additional underwater transducer to produce a specific sound field, and some have been used in conjunction with bubble diffusers with ambiguous results. Our measurements quantify the acoustic properties, including sound pressure level and frequency, generated by a fine- and coarse-bubble diffuser; which was used to compare with the audiogram for carp (response curve for sound detection). No behavioral tests isolated specific physical fields or sensory systems were performed in this stage of research, so the full impact of acoustic stimuli independent of hydrodynamic stimuli is unclear.

A basic understanding of sound properties and measurements techniques is important to review prior to presenting the results. A sound wave is a longitudinal wave, in which particles are displaced parallel to the direction of the motion of the wave (i.e. the particles oscillate locally). The frequency of the wave oscillations is one of the more prominent properties of sound, and is measured in cycles per second (Hz). The other prominent property of a sound wave is the acoustic pressure (P) or magnitude of the sound pressure wave. Acoustic pressure, generally reported in kPa, is merely the product of the particle velocity, speed of sound in a given medium, and the medium density; which is easily measured by electronic equipment such as hydrophones. Hydrophones capture a sound waveform which is viewed in the time-domain. A Fourier transformation of the waveform allows the sound wave to be viewed in the familiar frequency domain, in which the amplitude of the sound wave is plotted dependently of individual frequencies [Brigham, 1974;Ramirez, 1985]. At various locations along the flume (Figure 2-3), four 10-sec time-series sound signals are captured and transformed to the frequency domain. Once each sample is transformed, the average of the four 10s samples is used to describe the

sound at each measurement point. These plots also introduce the decibel (dB), a common unit of measure for sound pressure level. A decibel is a logarithmic ratio of the measured sound pressure amplitude to a reference pressure (for underwater measurements in this paper all decibels are referenced to 1µPa). To give an idea of scale, a 20 dB increase is equal to a 10 times increase in pressure. Figure 2-15 displays a typical SPL spectral density plot for background and with the diffuser on, indicating key features of the sound signal. The spectral density plots were generated by performing a Fourier transform of the time series waveform captured by the hydrophone. A spectral density plot allows for the sound signal to be inspected in the frequency domain, instead of the time domain. The background sample was taken with no flow through the flume and most laboratory noise was isolated to less than 100 Hz. The maximum SPL of 105 dB occurs between 200-300 Hz; while the SPL less than 100 Hz is mostly due to water motion noise on the hydrophone, and is classified as "pseudo-noise". In many cases the low frequency sound with the diffuser off was approximately equal to the SPL with the diffuser on. This may indicate that the signal could be instrument noise or a characteristic of the flume, similar to the flume experiments of Tonolla et al. [2009]. The resonant frequency is a characteristic of the flume size, and indicates that any sound at a lower frequency can not propagate within the flume [Akamatsu et. al, 2002]. Figure 2-15 is the SPL spectral density plot of the fine-bubble diffuser, which using equation (2-1), generates 1-2 mm bubbles that have a bubble resonant frequency of 3000 Hz (not indicated on Figure 2-15). The SPL for this sample happens to be at a lower frequency, indicating that for the fine-bubble diffuser the dominant frequency is a result of bubble formation rate and not the bubble formation itself.

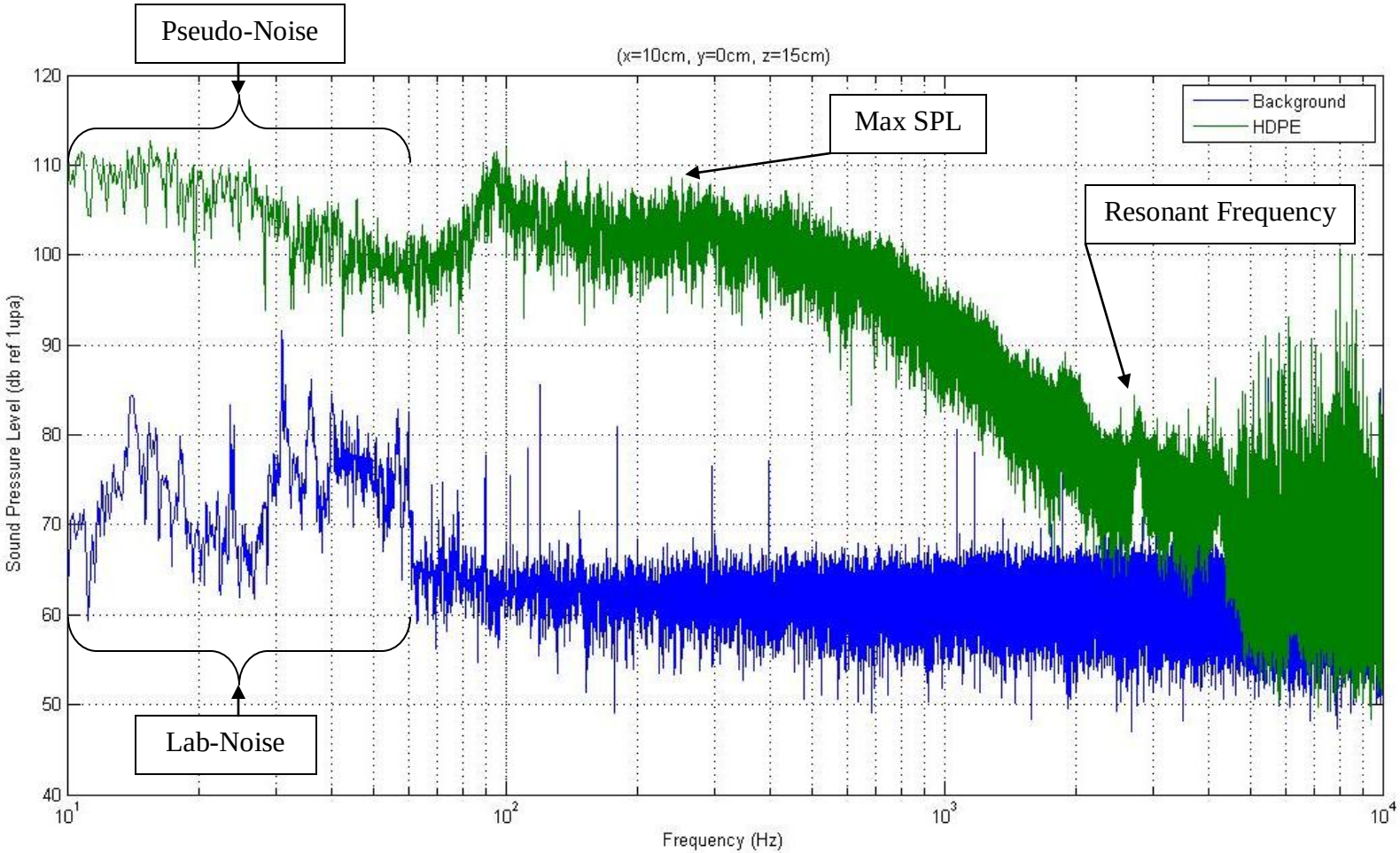

Figure 2-15. Typical SPL spectral density plot, highlighting key features

Note in Figure 2-15, the fine-bubble diffuser generates a sound approximately 40 dB greater than background noise at a particular location within the hearing range of carp (100-500 Hz). The maximum SPL, within the most sensitive region of carp hearing (100-500 Hz), was extracted from the data at each measurement location; this was done for background and diffuser on tests. Contour plots of the difference between diffuser on and background where created to demonstrate the range of influence of the diffuser on acoustic fields. Figure 2-16 provides a contour plot of the SPL above background for the fine-bubble diffuser at an air flow rate of 2.5 $Ls^{-1}m^{-1}$. Note the sharp gradient of SPL in the x-direction away from the barrier and location of the 10 dB contour indicating a zone of influence of approximately +/- D.

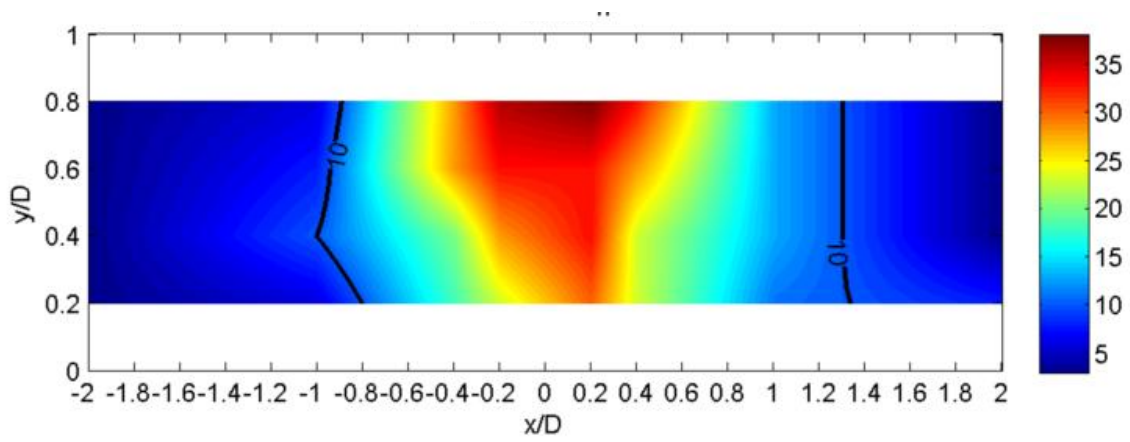

Figure 2-16. SPL above background for fine-bubble diffuser at a depth D=25 cm (scale is in dB)

Figure 2-17 displays the SPL above background for the coarse-bubble diffuser at an air flow rate of 2.5 $Ls^{-1}m^{-1}$.

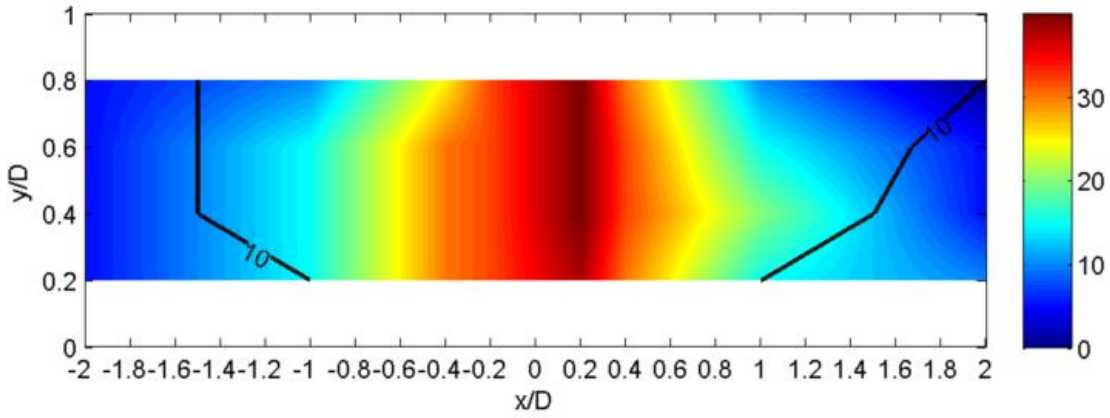

Figure 2-17. SPL above background for coarse-bubble diffuser at a depth D=25 cm (scale is in dB)

It is important to note that sound measurements in a confined tank will vary from tests in an unconfined domain (i.e. shallow water in circular tank with radius sufficiently large). Low frequency sound is subject to a "cutoff phenomena" which states that sound at a frequency less than the cutoff frequency will attenuate rapidly; while a sound at a frequency higher than the cutoff frequency attenuates slowly, but may be subjected to scattering and absorption [Urick, 1975]. Attenuation is defined as a signal strength loss of 20 dB after a certain length, the attenuation length. The cutoff frequency in a confined flume is equal to the resonant frequency of the flume, and Akamatsu et al. [2002] demonstrated that sound at a frequency equal to the resonant frequency can theoretically propagate indefinitely. Akamatsu et al. [2002] also constructed the following theoretical formulas to predict the resonant frequency of a specific tank size and attenuation length for any frequency. The cutoff frequency for a rectangular tank is:

$$f_{cutoff}^{rect} = \frac{c}{2}\sqrt{\left(\frac{1}{L_y}\right)^2 + \left(\frac{1}{L_z}\right)^2} \qquad (2\text{-}10)$$

Where

$L_{y,z}$ = dimensions of rectangular tank in y- and z-directions

Equation (2-10) is valid for a rectangular tank in which the length of the tank in the x-direction is sufficiently large. The cutoff frequency in an unconfined domain changes to:

$$f_{cutoff}^{circ} = \frac{c}{2h} \qquad (2\text{-}11)$$

Where

h = depth of water

Comparing equations (2-10) and (2-11) it is clear to see that the cutoff frequency in a rectangular tank will be greater than in an unconfined domain of the same depth. The rectangular flume at SAFL has a cutoff frequency of 3350 Hz and 2100 Hz for depths of 25 and 50 cm, respectively; conversely an unconfined domain at similar depths would have cutoff frequencies of 1500 Hz and 3000 Hz. The attenuation length, or length at which a 20dB decrease is experienced at a given frequency, is calculated using the previously calculated cutoff frequency:

$$D_{atten} = \frac{(2\ln 10)c}{4\pi} \frac{1}{f_{cutoff}\sqrt{1-\left(\frac{f}{f_{cutoff}}\right)^2}} \qquad (2\text{-}12)$$

Where

f = any given frequency

Equation (2-12) is valid for all frequencies but the cutoff in which no attenuation length is available. Figure 2-18 demonstrates the attenuation of a 500 Hz sound signal generated by the fine-bubble diffuser, at an air flow rate of 2.5 $Ls^{-1}m^{-1}$, plotted along with the theoretical attenuation. Note approximately at a distance equal to one depth away from the diffuser, the signal has nearly vanished at all depths. "U/S" designates upstream direction. Using equations (2-10) and (2-12) the expected attenuation length for the 500 Hz signal is 16.6 cm (x/D = 0.66).

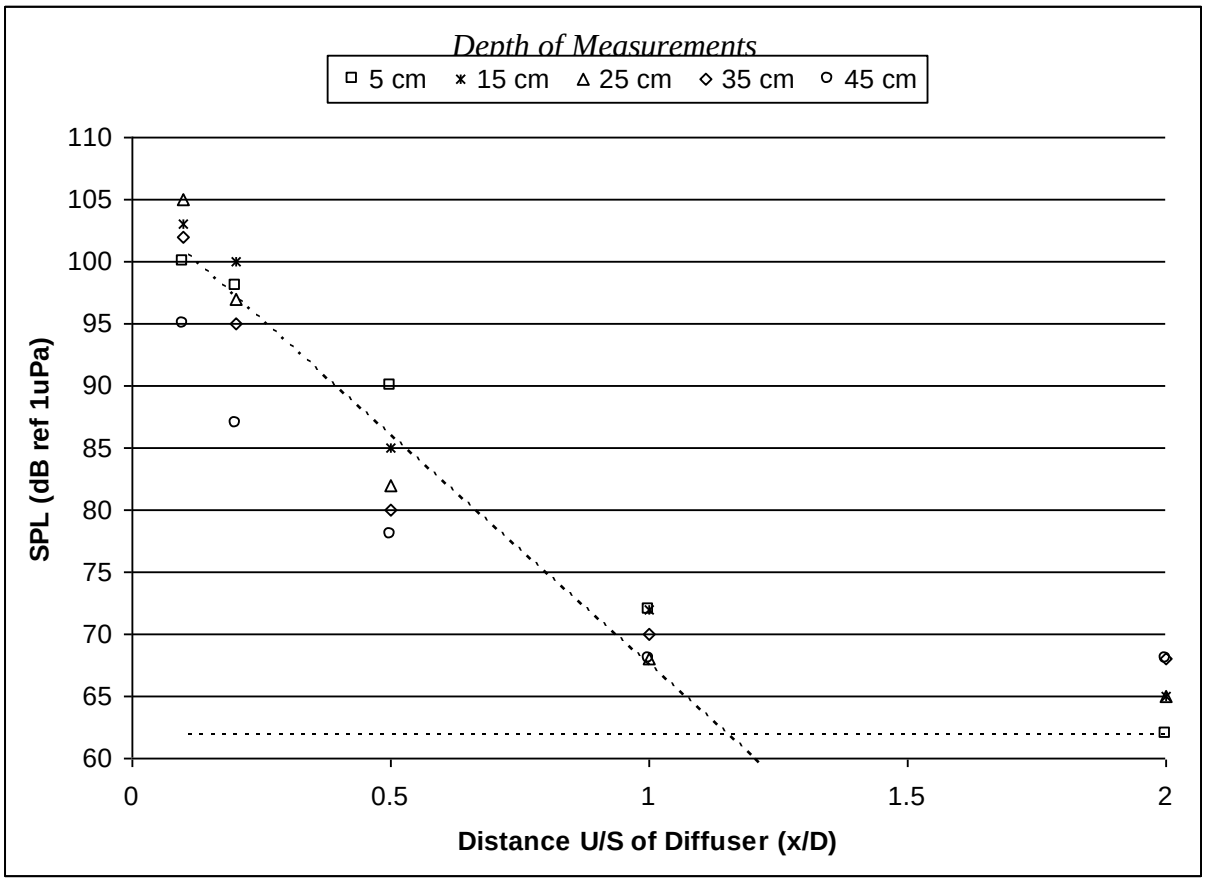

Figure 2-18. Attenuation plot for fine-bubble diffuser at depth D = 50 cm

The rapid attenuation of the primary sound signal is important to highlight, as this creates a natural gradient. Attenuation at lower frequencies also prevents the sound generated from the barrier to be broadcast a significant distance upstream or downstream of the barrier, potentially allowing carp to acclimate to the sound. The primary site for this barrier technology is in water less than 1m deep, meaning that sound less than approximately 1000 Hz will attenuate rapidly from any source (bubble or transducer).

Overall the acoustic field generated by each diffuser at varying flow rates and depths was quantified. Table 2-2 provides the maximum SPL within 100-500 Hz and distance at which a 10 dB increase over background is observed. The individual SPL plots of each diffuser could also be used to calculate the bubble oscillation amplitude from equation 2-2. The bubble oscillation was constant for each type of diffuser, which is expected as the bubble size remained constant for each test. The bubble oscillation for the fine-bubble diffuser, assuming a 1mm diameter bubble was 0.001mm, while the coarse-bubble diffuser, assuming a 5mm diameter bubble was 0.3mm.

Table 2-2
Maximum SPL of each diffuser

Diffuser Type	Flow-rate ($Ls^{-1}m^{-1}$)	Depth (cm)	Maximum SPL (dB)	Influence Distance (x/D)
Fine-Bubble	1	25	90	+/- 0.6
	2.5	25	100	+/- 1.0
	2.8	25	112	+/- 1.6
	2.5	50	98	+/- 0.6
	2.8	50	110	+/- 1.2
Coarse-Bubble	2.5	25	120	+/- 1.6
	2.8	25	125	> +/- 2.0

Chapter 3.0 Barrier Design and Development

The primary goal of the barrier design was to develop a configuration of diffusers that would generate a robust bubble curtain capable of deterring juvenile carp recruitment that could be scaled-up to use at real channels. Three barriers (Mark I – III) were developed, ranging from a single diffuser wand to multi-diffuser grid. Each barrier was designed to progressively increase the intensity of the bubble curtain influence, with the Mark III barrier reaching a maximum air-supply relative to scale-up feasibility. The barriers were all tested using the passive integrated transponder (PIT) tag detection system developed for the University of Minnesota's Aquaculture Center. This section outlines the laboratory setup, design of the bubbler barriers and lists the characteristic properties of each.

3.1 Laboratory Setup – Aquaculture Center

The Aquaculture Center facility features a circular tank constructed from setting a 1 m diameter tank inside a 3 m diameter tank. Air is supplied through the use of portable air-compressors and regenerative blowers. The blowers provide a large volume of air at low pressures, while the air-compressors supply a small volume of air at high pressures. Water flow is generated by a one inch diameter inlet pipe, pointed in a counter-clockwise direction. Select physical field measurements can be obtained through the same instrumentation used at SAFL.

The key component of the Aquaculture Center testing is the controlled experimental environment which tracks fish movements automatically through the use of radio frequency identification

(RFID) PIT tags. A PIT tag consists of a microchip that contains a unique identification number that can be detected/recorded passively when passing through a specifically tuned antenna. Each antenna is made of wire wound in loops and connected to tuner boxes, which are in-turn connected to a reader. The reader sends out a signal that allows each individual antenna to detect if a PIT tag is within its sensing range. The sensing range can be manually adjusted via wire thickness, number of loops, and fine tuning of the tuner box. The antenna used in the experimental tank have a reading range at approximately one meter, meaning a PIT tag within 0.5 m up- or down-stream of the antenna will be detected. The PIT tag reader system was provided by OregonRFID. Four antennas are evenly spaced around the test tank as seen in Figure 3-1. The antennas are numbered sequentially 1 through 4.

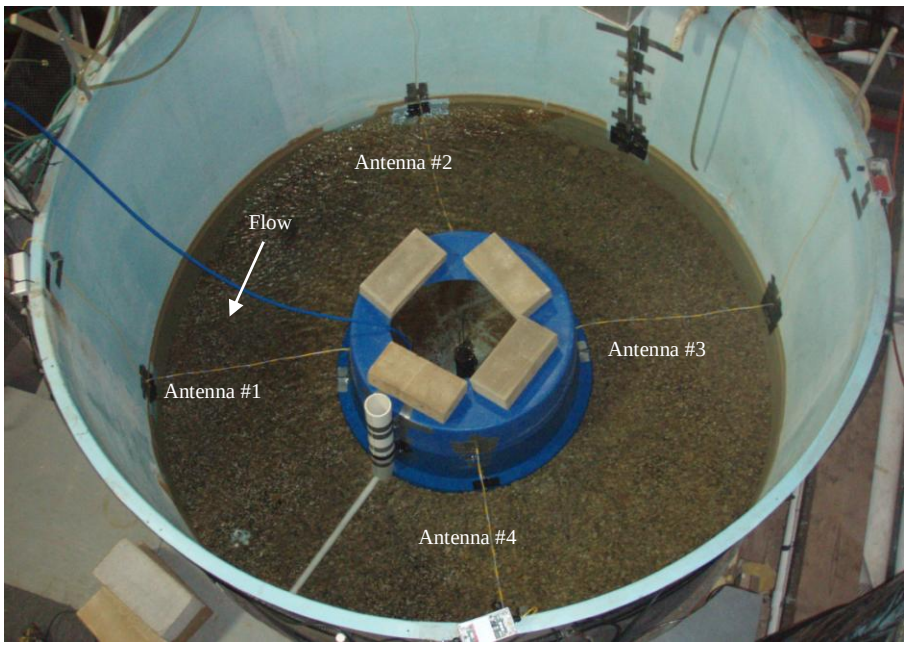

Figure 3-1. Experimental Setup of Circular Tank at the Aquaculture Center

The reader logs all detections onto a memory card which is downloaded via computer program Procomm Plus. Each detection log includes the date, time, PIT identification number, length of

consecutive detections, and location of detection, from which the number of times a carp passes in an up- or down-stream direction (i.e. 1-4-3 or 3-4-1) can be calculated. The exact location of the antennas to the barrier location varies per experiment and will be discussed in a later section.

Juvenile carp were selected randomly for PIT tagging, where each selected fish was tagged internally with a 23mm-long PIT tag. The tag was placed inside the body cavity via a ≈5mm incision located between the pectoral fins. The fish were anesthetized using tricaine methanesulfonate (MS222), and the incision was left to heal naturally. No mortalities were noted during the tagging process. The fish were allowed to recuperate at least three weeks before being tested. Only one PIT tagged carp is allowed in the test tank at a time, as multiple PIT tags cancel each other if in the same detection range simultaneously. The only way a PIT tag will not be detected, once the system is tuned correctly, is if the tag is oriented within 10 degrees of parallel to the antenna.

3.2 Mark I Barrier

The initial Mark I barrier tested at the Aquaculture Center was a single wand fine-bubble diffuser. Testing an individual wand served a dual purpose of being a starting point for barrier design and prototype experiment for the PIT tag detection system. The porous material utilized by the fine bubble diffuser is novel to bubble barrier designs based on the limited number of designs described in literature [Dawson et. al., 2006; Taylor et. al., 2005; Welton et. al., 2002]. An electric air-compressor was used to supply air to the wand at a maximum rate of approximately 1.0 $Ls^{-1}m^{-1}$. A single wand at such a low pressure did not create a very robust

barrier, resembling the typical aquarium air stone rather than impressive barrier. Upgrading the air supply to a gas powered air-compressor allowed a maximum sustained air-flowrate of 2.5 $Ls^{-1}m^{-1}$, similar to that tested at SAFL. Figure 3-2 provides the top view of single fine-bubble diffuser at an air-flowrate of 2.5 $Ls^{-1}m^{-1}$. The acoustic field generated by the Mark I barrier was confirmed with hydrophone measurements to be similar to that studied at SAFL.

Figure 3-2. Top view of Mark I barrier at 2.5 $Ls^{-1}m^{-1}$

The Mark I barrier appears to have retarded carp movement but not limit the number of passages through the barrier. A complete discussion of barrier test results is available in a later section.

3.3 Mark II Barrier

Due to the relatively minimal effect of the Mark I barrier on carp movement, a sizable increase in dimension, gradient, and air-flowrate was integrated into the design of the Mark II barrier. The design of the Mark II barrier also focuses on the hypothesis that the acoustic field is the primary agent for limiting carp passage; therefore, a gradient of SPL was created in the downstream

direction by using a combination of different diffusers. The Mark II barrier consisted of the following (looking up- to down-stream): one fine-bubble diffuser supplied by gas-powered compressor, four coarse-bubble diffusers supplied by regenerative blowers, and one ultra-coarse diffuser (3 mm diameter holes spaced at 5 cm) also supplied by regenerative blowers. Figure 3-3 provides a diagram of the Mark II barrier configuration.

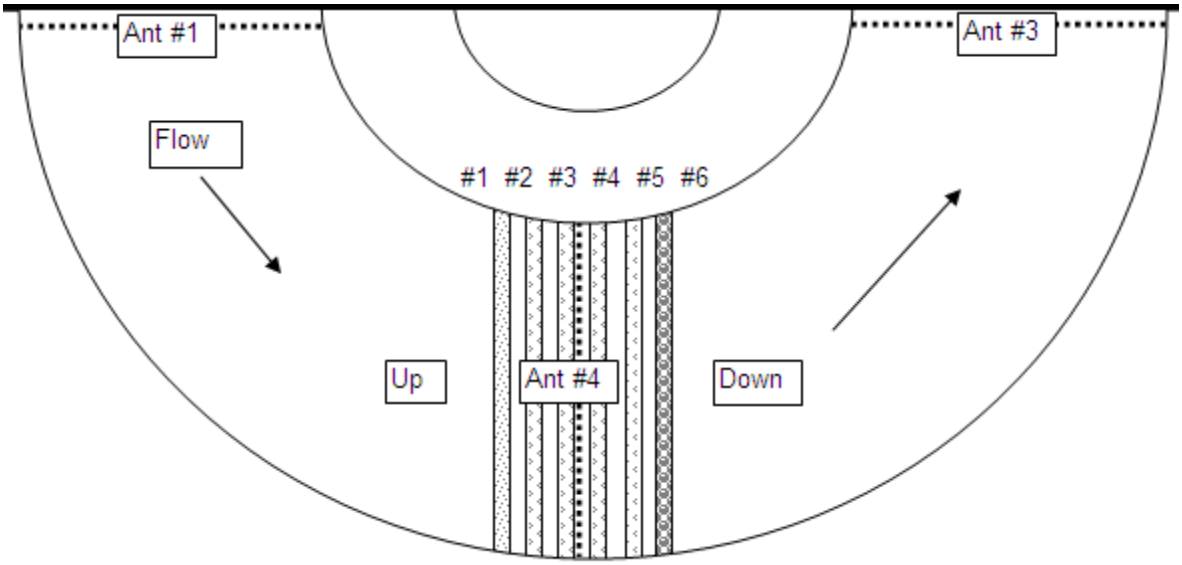

Figure 3-3. Diagram of the Mark II barrier in the Aquaculture Center

The air flow to diffuser #2 to #5 is controlled by a PVC manifold capable of directing the quantity of air to each diffuser. The regenerative blowers are capable of supplying greater amounts of air at low pressures. The total air-flowrate supplied to the entire Mark II barrier is 31.5 $Ls^{-1}m^{-1}$, approximately a 10 times increase of the Mark I barrier. The Mark II barrier thickness also increased from approximately 10-15 cm to almost 1 m.

The SPL generated by the barrier without the fine-bubble diffuser was measured by placing the hydrophone 10 cm upstream of #2 (indicated as US) and 10 cm downstream of #6 (indicated as DS). While maintaining the location of the hydrophone constant, multiple combinations of diffusers were tested to find the optimal sound field. Figure 3-4 presents the SPL at 150 Hz, 10 cm up- and down-stream of the diffusers incrementally adding or removing selected diffusers.

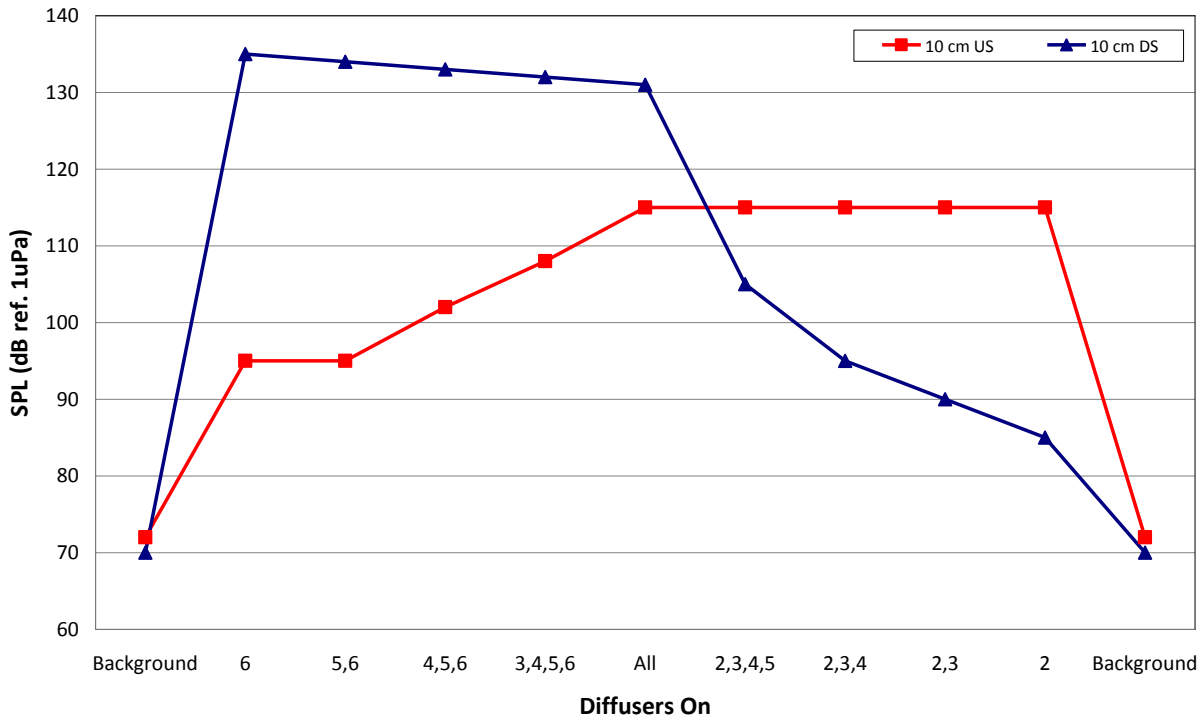

Figure 3-4. SPL of Mark II barrier without fine-bubble diffuser

Note the maximum SPL of 135 dB occurs only when the ultra-coarse diffuser is supplied all the air; however, only a 4 dB decrease is observed when the air is distributed between all 5 diffusers. The constant SPL generated near the edge of the barrier indicates that the SPL on the up- and down-stream sides of the barrier is controlled by each respective exterior diffuser. The optimal setting was selected to be the full air supplied to all diffusers, as this creates the strongest SPL

throughout the entire barrier. Adding the fine-bubble diffuser increased the complexity of flow fields, and extended the SPL on the up-stream side of the barrier at 100 dB. Figure 3-5 provides a top view of the Mark II barrier with and without air supplied.

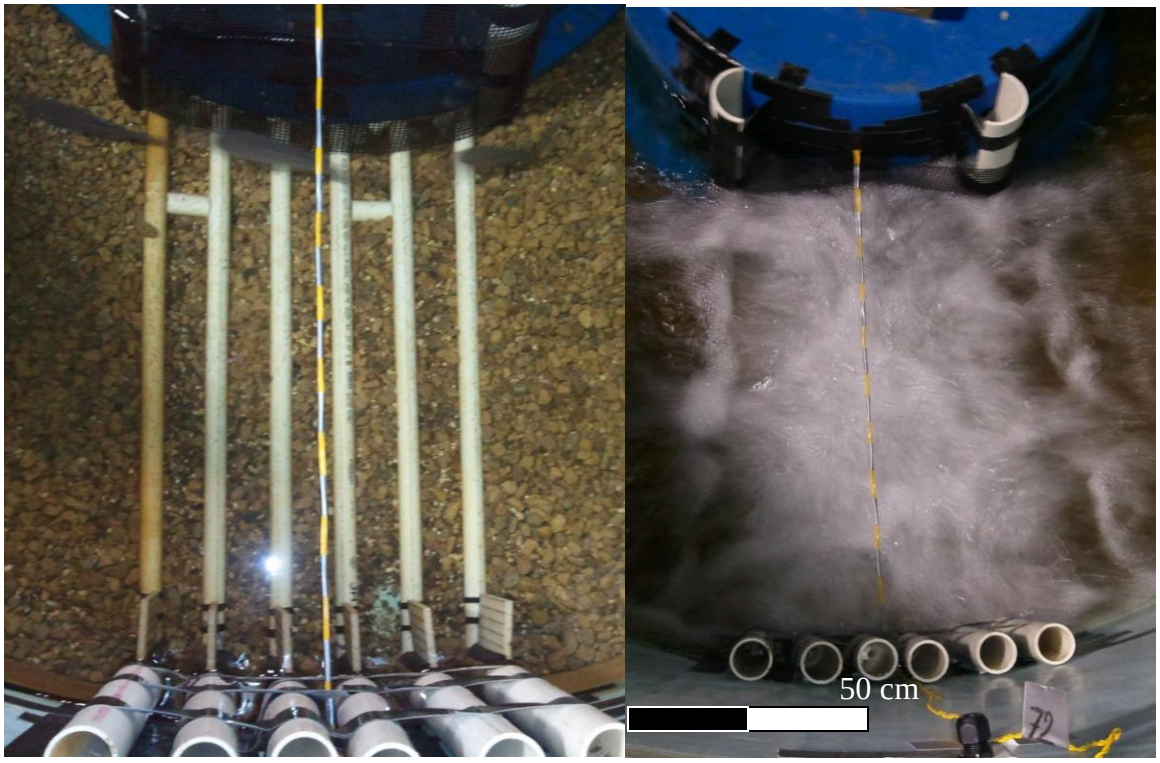

Figure 3-5. Top view of Mark II barrier without (left) and with air (right)

5.3 Mark III Barrier

The Mark III barrier was designed to maximize the air-supply equipment available at the Aquaculture Center; this also corresponds to a maximum air-supply that can be effectively scaled-up to an existing channel. The design of the Mark III barrier focuses on the hypothesis that the acoustic field is the primary agent for limiting carp passage as the velocities generated by the bubble barrier are not significantly greater than naturally occurring velocities in a flashy

stream. In contrast to the Mark II barrier, the Mark III barrier is characterized by a constant air flow over a uniform barrier; therefore, the SPL is constant from the up-stream to down-stream sides. Figure 3-6 displays the typical layout of the Mark III barrier. The Mark III barrier consists of PVC pipe containing ultra-coarse holes (3 mm diameter holes spaced at 2.5 cm) with a pipe grid spacing of 12.5cm X 16.5cm. The ultra-coarse holes were selected to provide the highest SPL while not reducing the air-pressure to a point of non-uniform bubble curtains. The PVC grid is separated into four individual quadrants, each supplied by a single regenerative blower. The total air-flowrate supplied to the entire Mark III barrier is 108 $Ls^{-1}m^{-1}$, approximately a 3 times increase of the Mark II barrier. The Mark III barrier thickness remained consistent with the Mark II barrier at 1m. An interesting feature of the Mark III barrier is the individual cells of bubble curtains created by the grid layout. The bubble cells provide a labyrinth configuration of curtains that removes any gaps that carp could possible navigate through, i.e. the carp must pass through a bubble curtain.

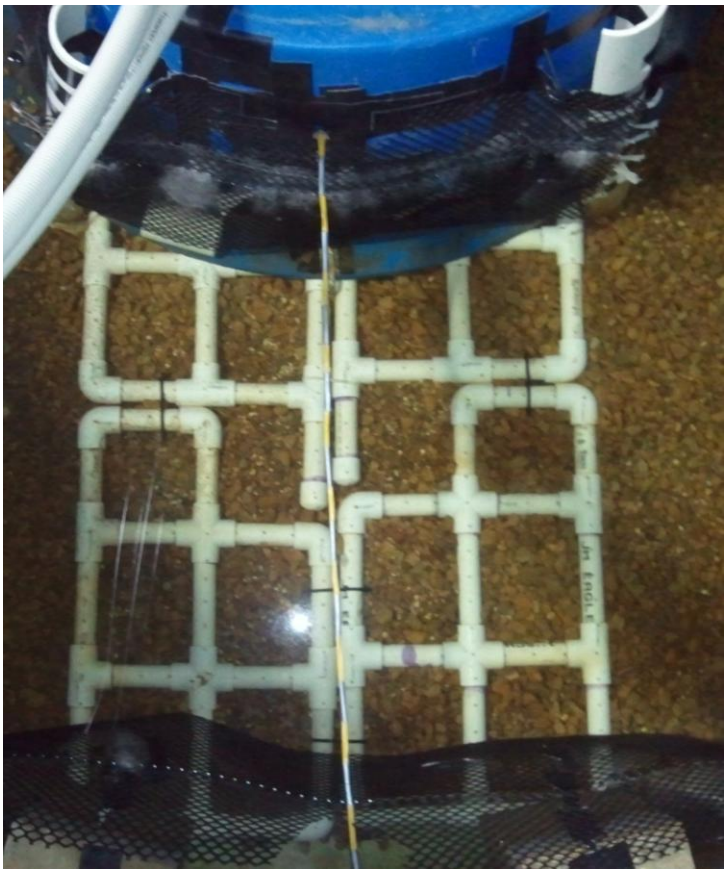

Figure 3-6. Mark III configuration (no air supplied)

The SPL generated by the barrier was measured by placing the hydrophone 10 cm upstream and 10 cm downstream of the barrier. The maximum SPL generated up- and down-stream is approximately 124 dB, which is approximately 40 dB higher than background. The SPL was also measured in the rear section of the tank to be 85 dB, which at less than 10 dB above background falls within the "cocktail party" effect and should be undetected by carp. The Mark III barrier does not have an equivalent SPL field as the Mark II, approximately 10 dB drop on the down-stream side and 10 dB gain on the up-stream side. Maximum SPL reduction is the result of reduced blower efficiency and greater demand of air in each diffuser quadrant. Figure 3-7 provides a top view of the Mark III barrier with air supplied.

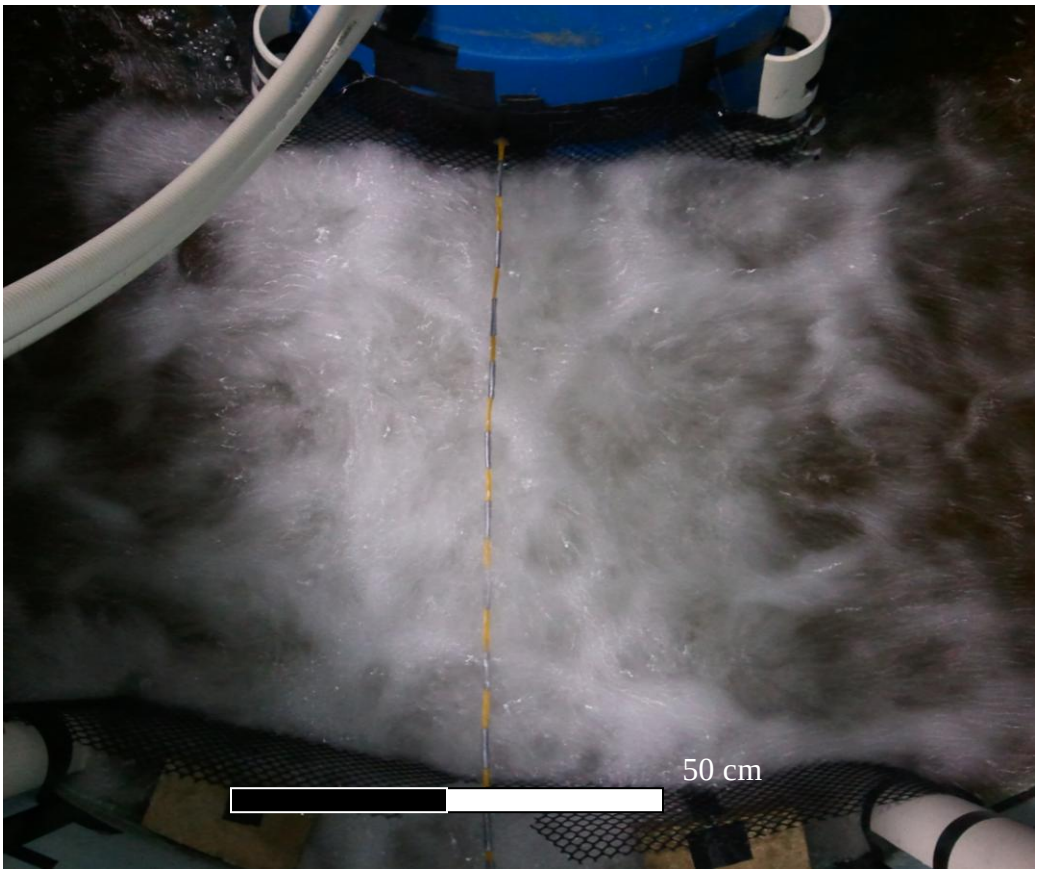

Figure 3-7. Top view of Mark III barrier and with air

Chapter 4.0 Testing of Barriers

4.1 Fish Testing Protocol

A strict testing protocol is paramount to reduce the number of variables that could influence carp behavior during a given testing period. Following the experiments by Zydlewski et al [2005], our tests will be carried out at the Aquaculture Center in a circular tank with PIT tag antenna evenly spaced in the channel. A moderate flow of 5 cm/s is generated in a counter-clockwise direction by a freshwater input. Water is continuously cycled through a re-circulation system via a drain separated from the fish by the central tank as seen in Figure 2-1. All experimental carp were caught in Lake St. Catherine, MN via electro-fishing in July 2010. All fish are maintained onsite in four separate tanks onsite; a separate tank for tagged/untested, tagged/tested, untagged/untested, and untagged/tested carp. All tanks are kept in darkness by placing tarps overtop and water is continuously re-circulated. The carp are fed pellets once a day at between 10:00 AM and 12:00 PM. Water temperature is maintained at approximately 21 degrees C in all tanks, to reduce any undue stress on the fish during testing. The juvenile carp used the Mark II and Mark III barrier tests weighed 204 +/- 77g and were 259 +/- 29mm in total body length. The carp used in the Mark I test were similar in size, but were lost due to disease between the Mark I and Mark II barrier tests.

Tests were carried out in complete darkness to remove any visual influence of the bubble curtain; tests occur between the hours of 10:00 PM and 6:00 AM, with a tarp covering the

test tank and all lights off in the laboratory. An attempt was made to randomly select fish from the untested populations, so as to generate independent results. Each test consisted of selecting one PIT tagged fish and two untagged fish and placing them in the test tank. The first 10min of each test was acclimation time, and not included in the data analysis. This time allowed fish to begin schooling and reduce stress due to handling. The test period encompasses the following 7 hours of detections. During the tests, all extraneous electrical systems were turned off, to reduce noise detected by the antenna. For every test completed with air supplied to the barrier, one control test was completed. A control test consisted of using a new group of fish in the test tank with the barrier in place, but not supplied air. Once the testing was complete, all fish are weighed and measured for total body length. The fish were then separated into holding tanks with other tested fish, for future tests. No fish was used in the test tank twice throughout the barrier on, or corresponding control, test for a given barrier type.

Carp used in the Mark II barrier trials were reused for the Mark III barrier trials. Fish were selected out of a population of fish that had previously been used in control and barrier-on tests. Each trial set was completed two month apart, to eliminate any experience gained from previous testing. One month after the Mark II barrier trials concluded, nine randomly selected carp were re-tested with the Mark II barrier-on to see if any previous experience with the barrier decreased the effectiveness. The results of this testing is available in Appendix A.

The detections are analyzed using the computer program Matlab and MS Excel to calculate the number of passages over the barrier, average passage time, number of detections at the barrier, and average time spent near the barrier. Due to the limited size and large variability in the data sets, the probability reported in the following sections comparing each barrier together is a result a bootstrap statistical analysis. The bootstrap method was ideal for the data sets collected as the variance and data set size varied greatly between tests. Via re-sampling with replacement of the original data, 95%confidence intervals and null hypothesis testing was determined for various combinations of data sets. A simple t-test and Mann-Whitney U-test were used to compare control and diffuser on tests of each individual trial, as noted.

4.2 Barrier Test Results

4.2.1 Mark I Barrier

The Mark I barrier tests have a dual objective of prototyping the PIT tag detection system and as a starting point for the barrier designs. The Mark I barrier was supplied an air flow rate of 1.0 and 2.5 $Ls^{-1}m^{-1}$. A total of four control tests, four barrier tests with 1.0 $Ls^{-1}m^{-1}$, and two barrier tests at 2.5 $Ls^{-1}m^{-1}$. A limited number of tests were completed as the entire test population was lost to disease. The PIT tag system produced accurate counts of fish passages as the number of missed detections was less than 1% of all detections. Detections are considered missed when the carp is detected at two non-

consecutive antennas. The control tests associated with the Mark I barrier had similar up-stream and down-stream movements. Figure 4-1 provides the total up-stream passages over the barrier for the control and two flow rates. Figure 4-2 provides the total down-stream passages over the barrier for the control and two flow rates. The p-values provided in Figure 4-1 and 4-2 are calculated by unpaired t-test. Note that there is a slight decrease in movements when the barrier is on in both directions, but is not statistically significant. Also note that all bar graphs are provided with standard error bars.

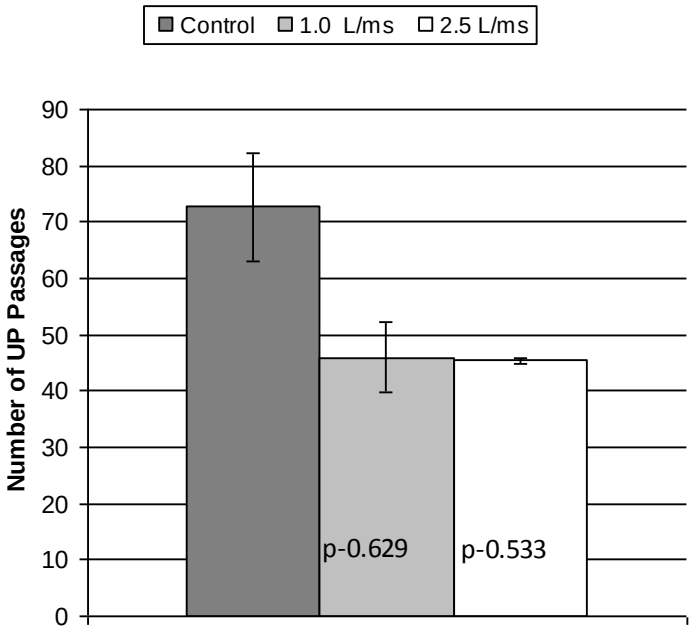

Figure 4-1. Number of up-stream passages over the Mark I barrier

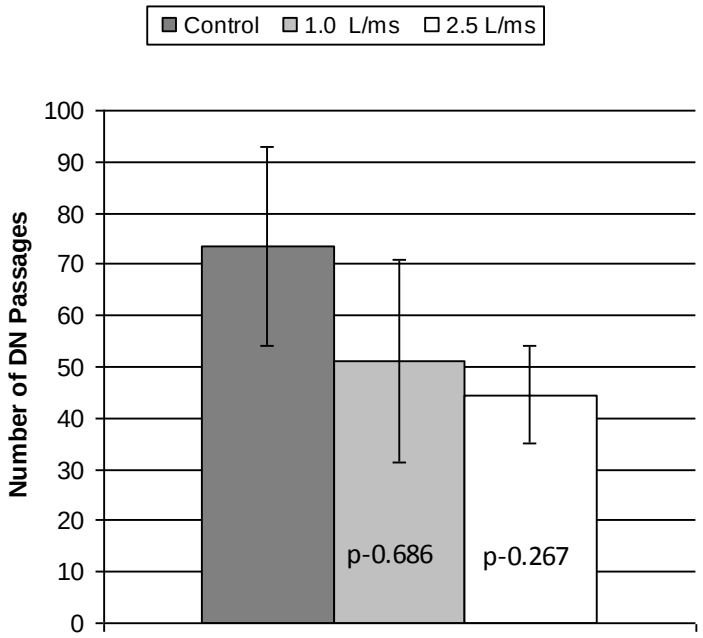

Figure 4-2. Number of down-stream passages over the Mark I barrier

Figure 4-3 and 4-4 provide the mean time required to pass over the barrier during the control and two flow rates. Note that the passage time increases for the barrier on configurations, and is statistically significant with $p < 0.05$.

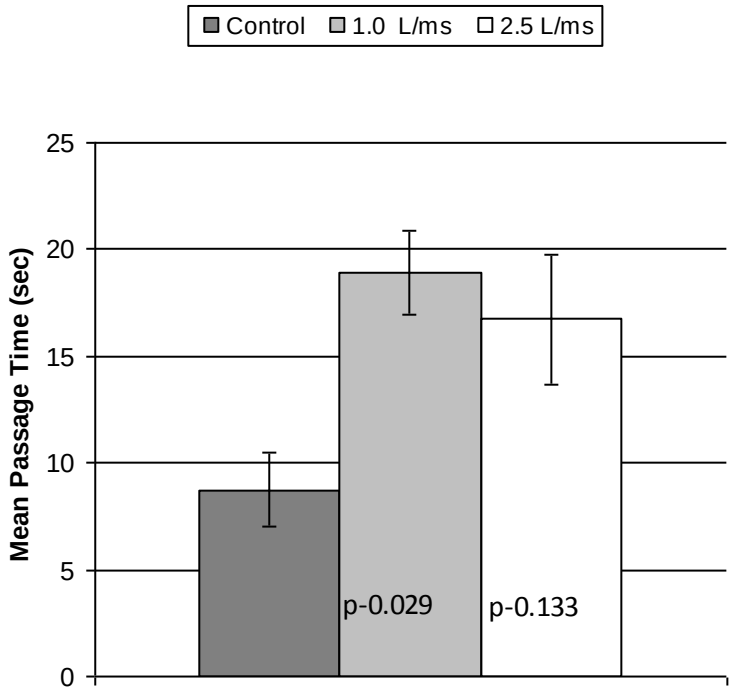

Figure 4-3. Mean passage time to cross Mark I barrier in the up-stream direction

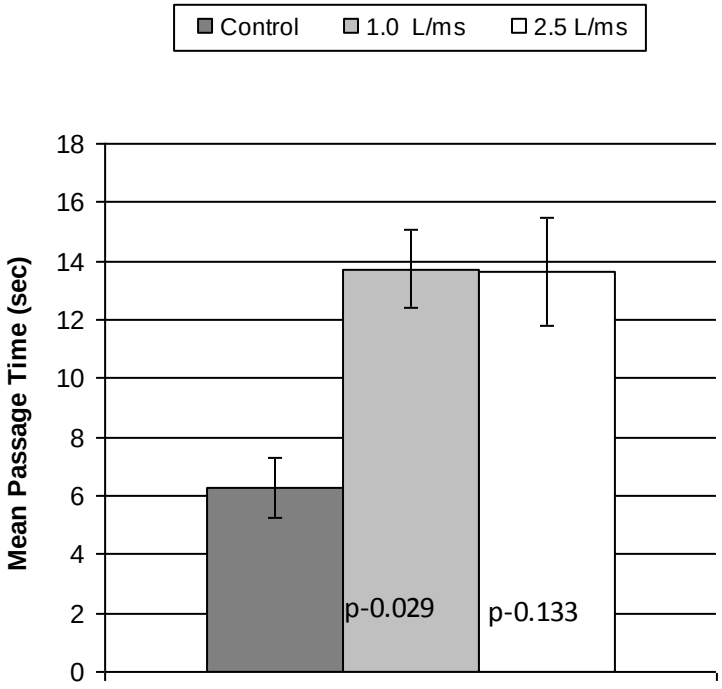

Figure 4-4. Mean passage time to cross Mark I barrier in the down-stream direction

The limited number of tests restricts the statistical significance of these results; however, the barrier tests indicate that the Mark I barrier may retard carp movement by approximately 10 seconds.

4.2.2 Mark II Barrier

The Mark II barrier discharges 10 times the air-supply as the Mark I barrier and represents a significantly more vigorous bubble curtain. A four antenna experimental configuration provides more information on the carp movements, as the antenna located directly over the barrier can detect the total time the carp spend near the barrier. Eight tests were performed with 31.5 $Ls^{-1}m^{-1}$ air flow rate and without air-supplied to the barrier. Figure 4-5 and 4-6 provide the total up- and down-stream passages over the Mark II barrier during the control and barrier tests. During the control experiments, the carp displayed a tendency to move in a net down-stream motion. The down-stream migration was expected as the carp could not orient with the substrate in total darkness. Note the decrease in passages is statistically significant using the Mann-Whitney U-test, indicating that the barrier does limit carp movement. Note that one barrier on experiments resulted in zero total passages.

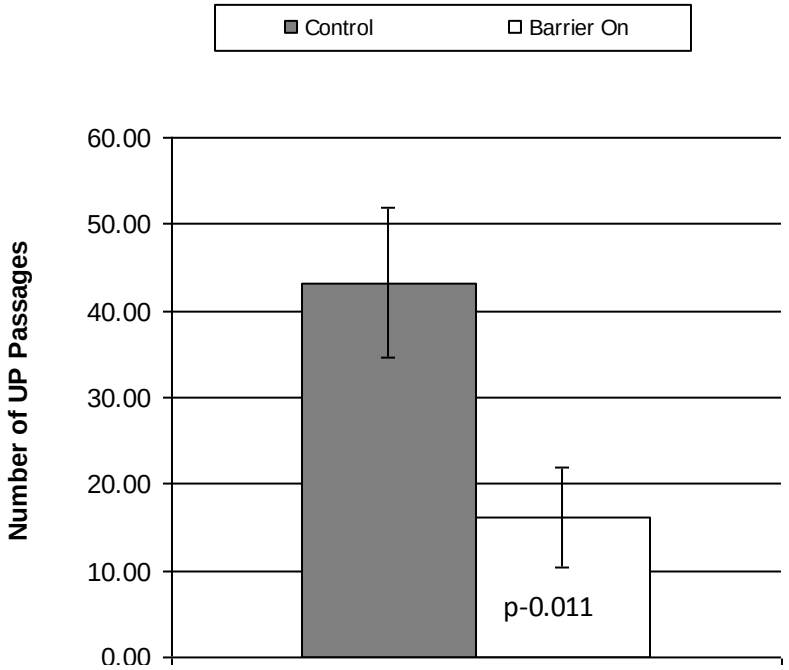

Figure 4-5. Total number of up-stream passages over Mark II barrier

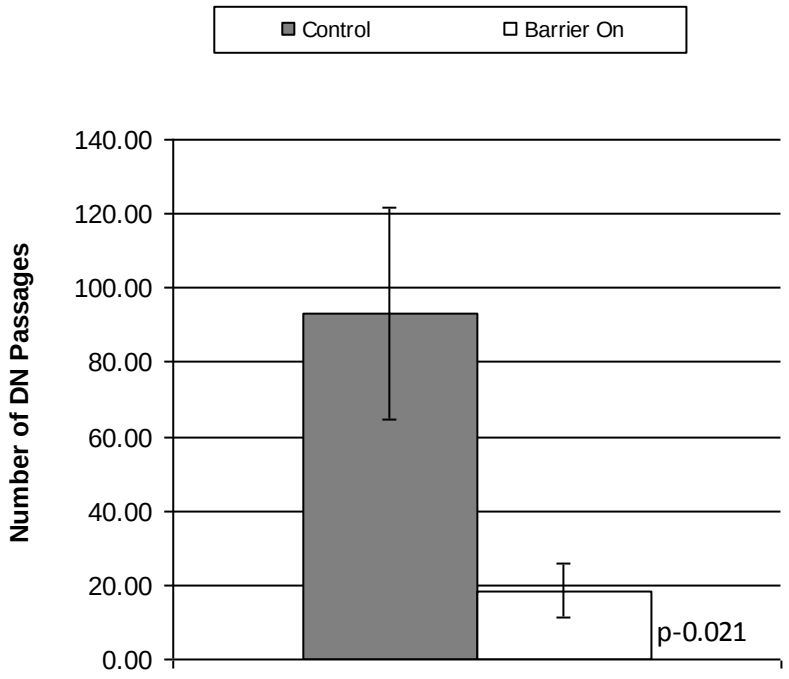

Figure 4-6. Total number of down-stream passages over Mark II barrier

Figure 4-7 displays the total number of passages between any two antennas as an indication of the relative activity of the carp being tested. Note the 30% decrease in total passages when the barrier is on is mildly statistically significant with p~0.05. The number of passages can be interpreted as a rate of movement by the carp over the testing period. During the control tests, the carp averaged 2 passages per minute, while that number decreased to 1.5 passages per minute with the diffuser on. The reduced number of passages between any two antennas could be a result of the reduction of passages over the barrier, which accounts for approximately 100 passages. Despite the reduced activity between control and barrier test, it is important to note the carp are consistently active in all tests.

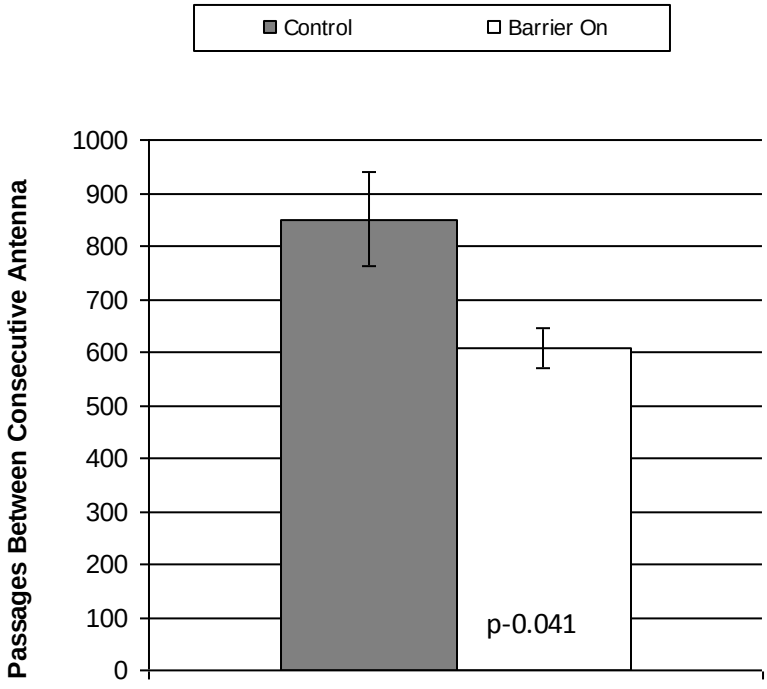

Figure 4-7. Total number of passages between any two consecutive antennas

Figures 4-5 and 4-6 clearly demonstrate the desired effect of the barrier on carp movment. Although the Mark II barrier does not completely stop all carp passage, it does decrease the number of passages in the up- and down-stream directions by approximately 60% and 80%, respectively. There was no statiscial difference between control and barrier tests in the passage time; however, this cannot be compared to the Mark I test results as the antenna configuration changed from 3 to 4 antennas. The bootstrap analysis was used to test the significance of the percentage of decreased passages over the Mark I and Mark II barriers. Figure 4-8 and 4-9 provides the results of the bootstrap analysis to see if the Mark II barrier is statistically different than the Mark I barrier in up-stream and down-stream passage reduction. Note that the error bars represtent the upper and lower bounds of the 95% confidence interval.

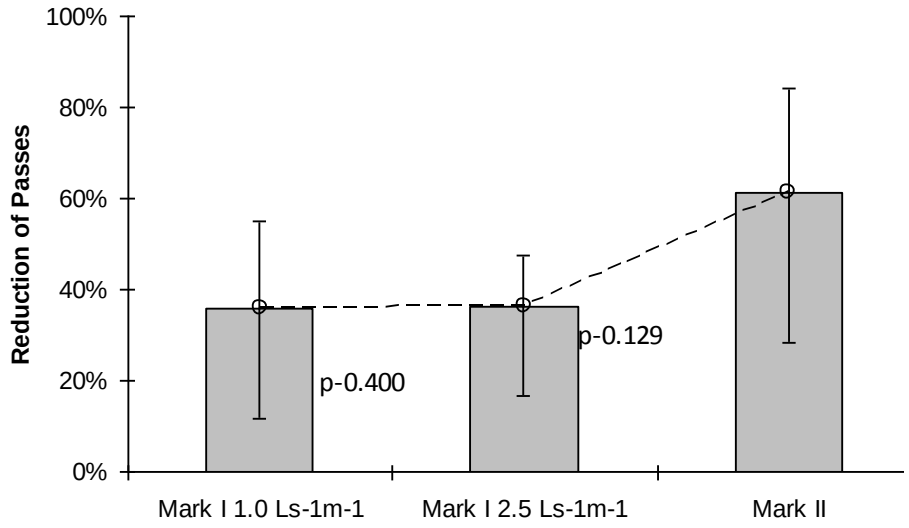

Figure 4-8. Comparison of Mark I and Mark II barriers for reducing up-stream passage

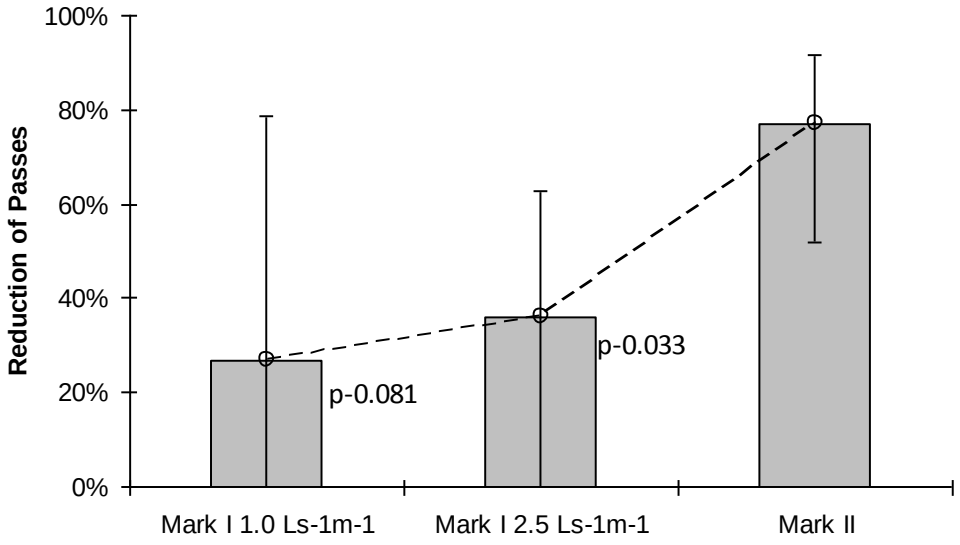

Figure 4-9. Comparison of Mark I and Mark II barriers for reducing down-stream passage

The Mark II barrier displays a sizable improvement over the single wand design of the Mark I barrier, increasing the effectiveness by approximately 45% and 20% in the down- and up-stream directions, respectively. The small data sets in addition to the large variance from the Mark I tests, reduces the reported p-value, but a relative measure of improvement is still observable.

4.2.3 Mark III Barrier

The Mark III barrier discharges three times the air-supply as the Mark II barrier and represents a maximum effort of supplying a complete bubble curtain. Similar to the Mark II tests, a four antenna experimental configuration tracked carp movements. The tests were slit between two separated tanks, to decrease total testing time. Each tank contained a Mark III barrier with full PIT tag tracking system. The readers were

synchronized per the manufacturer's instructions to reduce potential noise and interference. On each given night of testing one tank was selected as the test tank and the other the control tank. The selection of tanks was chosen at random with each tank being used an equal number of times for each experiment. A total of 7 tests were performed with 108 $Ls^{-1}m^{-1}$ air flow rate and without air-supplied to the barrier. Figure 4-10 and 4-11 provide the total up- and down-stream passages over the Mark III barrier during the control and barrier tests. Again, a net down-stream displacement was observed during the control experiments. Decreased passages ($P < 0.5$, Mann-Whitney U-test)indicated that the barrier does limit carp movement. Note there was one barrier on test that resulted in zero total passages.

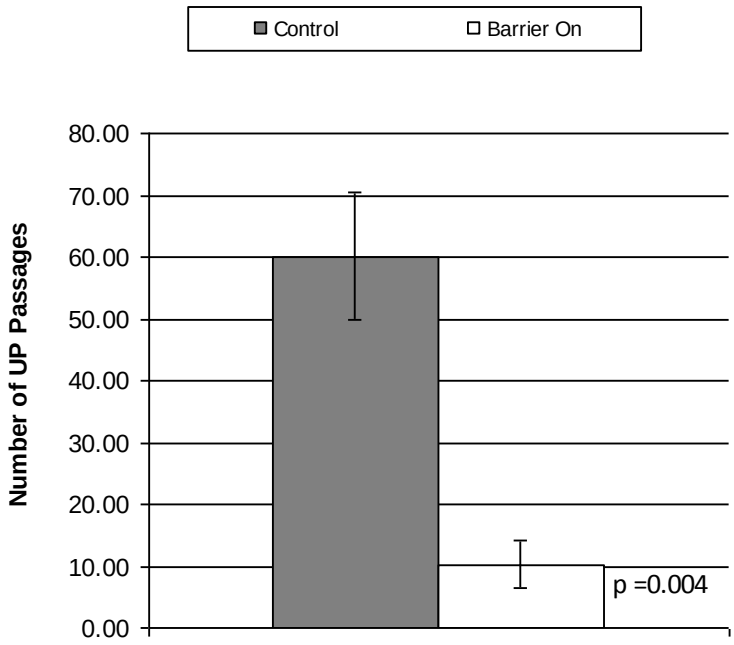

Figure 4-10. Total number of up-stream passages over Mark III barrier

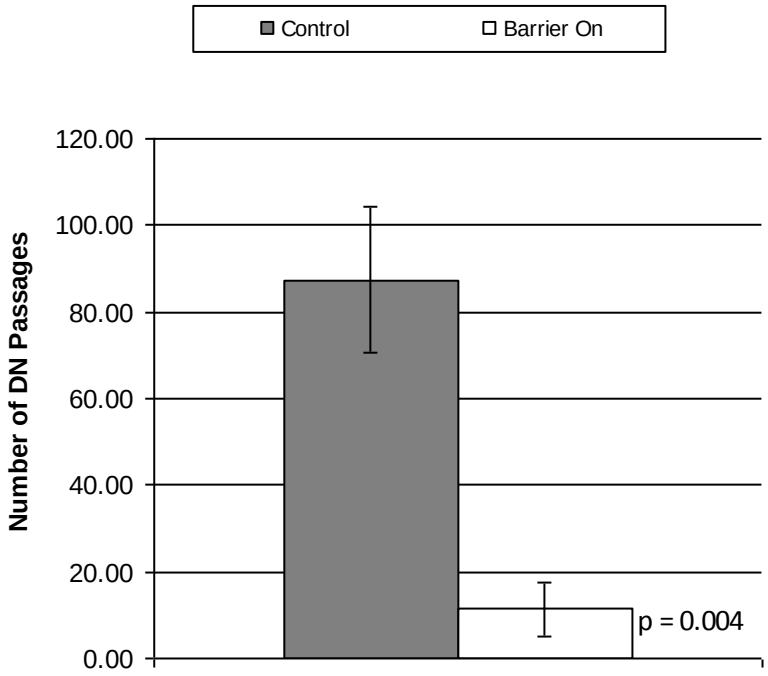

Figure 4-11. Total number of down-stream passages over Mark III barrier

Figure 4-12 displays the number of passages between any two consecutive antennas during the Mark III experiments. Using this as a measure of relative activity by the carp in a 7 hour span, it is clear that the carp remained active throughout the experiment process. The carp displayed 2.9 and 2.7 passages per minute during the control and diffuser on experiments, respectively. Note that the relative activity of carp during the Mark II and Mark III experiments is similar.

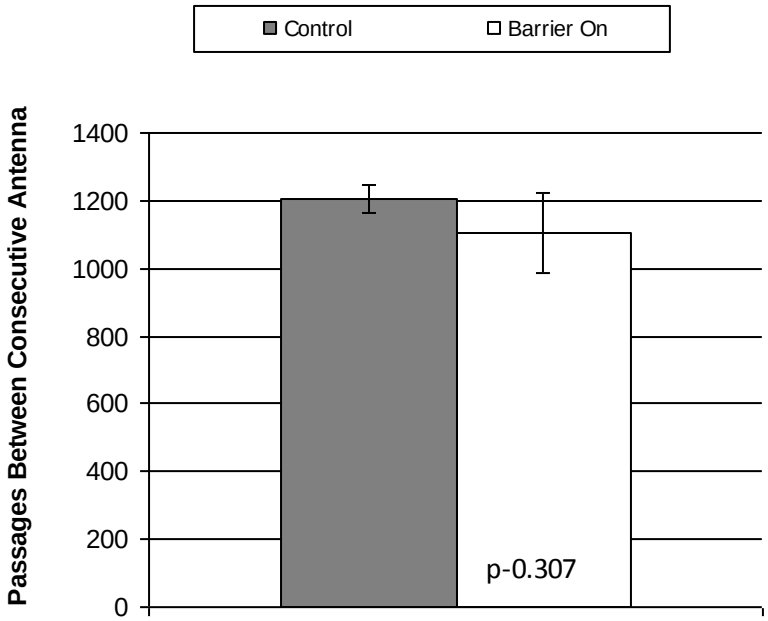

Figure 4-12. Total number of passages between any two consecutive antennas

Figures 4-10 and 4-11 clearly demonstrate the desired effect of the barrier on carp movment. The Mark III barrier does not completely stop all carp passage; however, it does decrease the number of passages in the up- and down-stream directions by approximately 83% and 87%, respectively. The bootstrap analysis was used to test the significance of the percentage of decreased passages over the Mark I and Mark III barriers and the Mark II and Mark III barriers. Figure 4-13 and 4-14 provides the results of the bootstrap analysis to see if the Mark III barrier is statistically different than the Mark I barrier for up- and down-stream passage reduction. Note that the error bars represtent the upper and lower bounds of the 95% confidence interval.

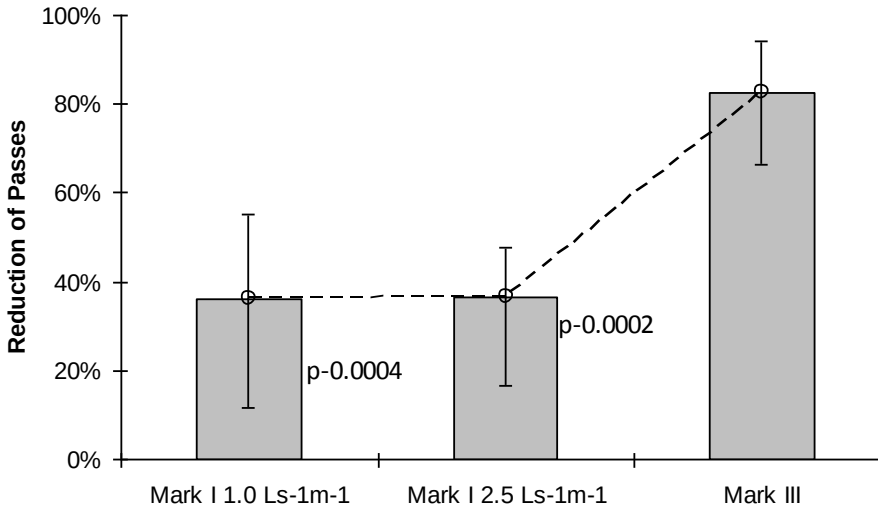

Figure 4-13. Comparison of Mark I and Mark III barriers for reducing up-stream passage

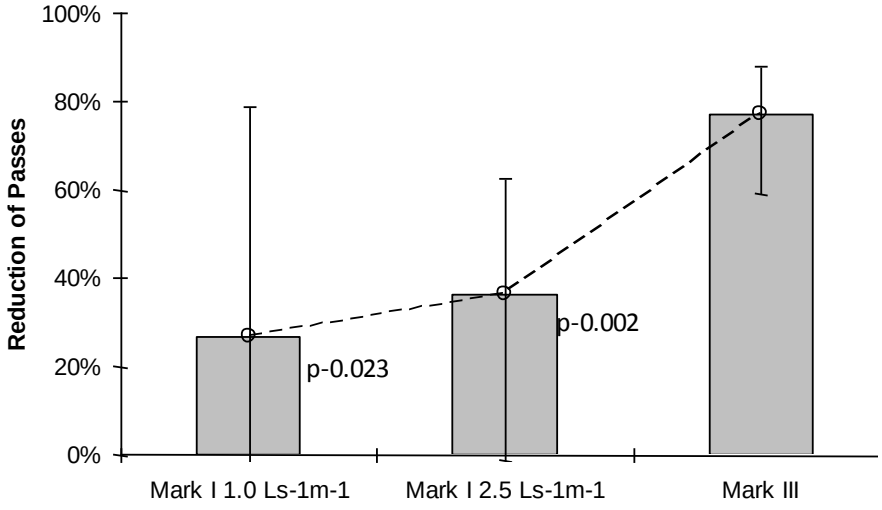

Figure 4-14. Comparison of the Mark I and Mark III barriers for reducing down-stream passage

The Mark III barrier is also a significant improvement over the Mark I barrier, increasing the effectiveness by approximately 50% and 40% in the down- and up-stream directions, respectively. The results are also statistically significant with $p<0.05$ for all cases. A similar analysis comparing the Mark II and Mark III barriers revealed no statistically

significant increase in effectiveness. The up-stream passage reduction comparison resulted in p=0.143, while the down-stream passage was p=0.402.

4.3 Modeling of Carp Movement

The data collected from the PIT-tag system can be useful in generating a spatial distribution model to describe individual carp movement. The spatial variance of carp movements during the control tests could provide a basis for a predictive model; while comparison of spatial variance between control and diffuser-on tests may indicate clear behavioral response. A spatial distribution model could eventually be used in a theoretical model incorporating hydrodynamic and acoustic models to determine what characteristic of the bubble barrier has the greatest influence on carp avoidance.

The relationship of spatial variance over time describes how carp spread out during the tests; a linear trend indicates that the movement follows a Brownian random walk, while a power-law trend indicates a Lévy random walk which is characterized by large step sizes [Metzler et al., 2000]. Anomalous transport, transport described by Lèvy random walks, have been used to describe various biological systems such as nematode movement [Hapca et al., 2007], leptokurtic distribution of stream fish [Zhang et al., 2007], and various others that all feature large step sizes or large wait times that do not fit a Gaussian distribution [Metzler et al., 2000].

The first step to obtaining the spatial variance, square deviation from the mean, of the carp dispersal data requires that a position time series be generated for each trial. The PIT tag system only records the position of the fish as it enters the reading range of one antenna, not the exact location at a set time interval. The data log must be transformed from a circular reference to linear reference to visualize the net movement during each trial. Whereas the barrier effectiveness tests only reported the crossings over the barrier in a certain direction, the position time-series will provide the net direction of movement. This is accomplished by assigning each passage between antennas with the centerline distance between antennas. Figure 4-15 and 4-16 provide the control and diffuser on test position time series data for the Mark II barrier. Note that a positive distance is in the downstream direction. Note that Control 3 in Figure 4-15 exhibits a significantly larger step size than the other data points.

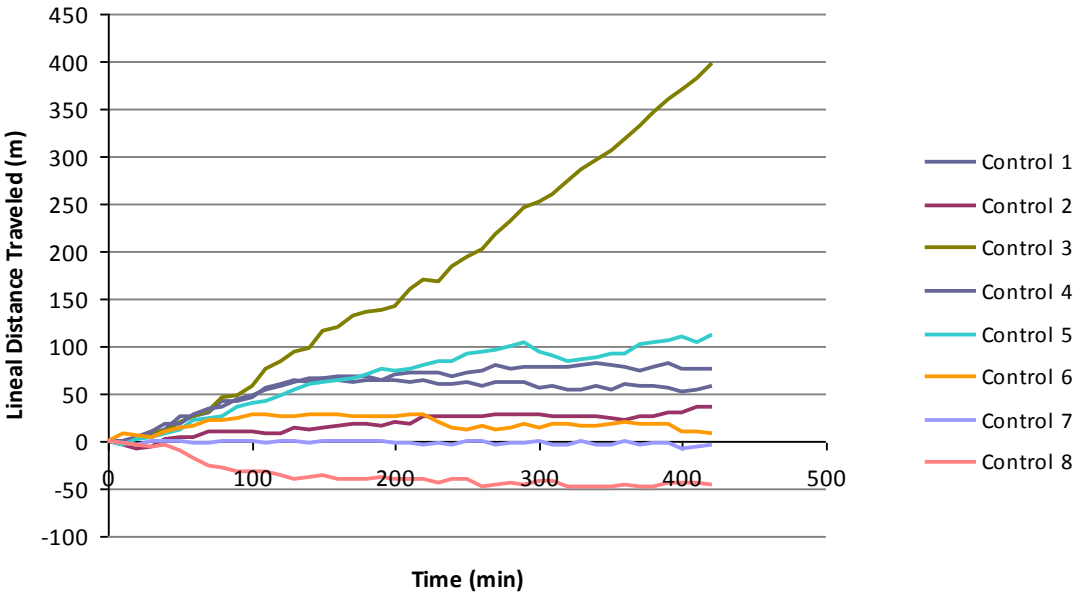

Figure 4-15. Position time series for Mark II control tests

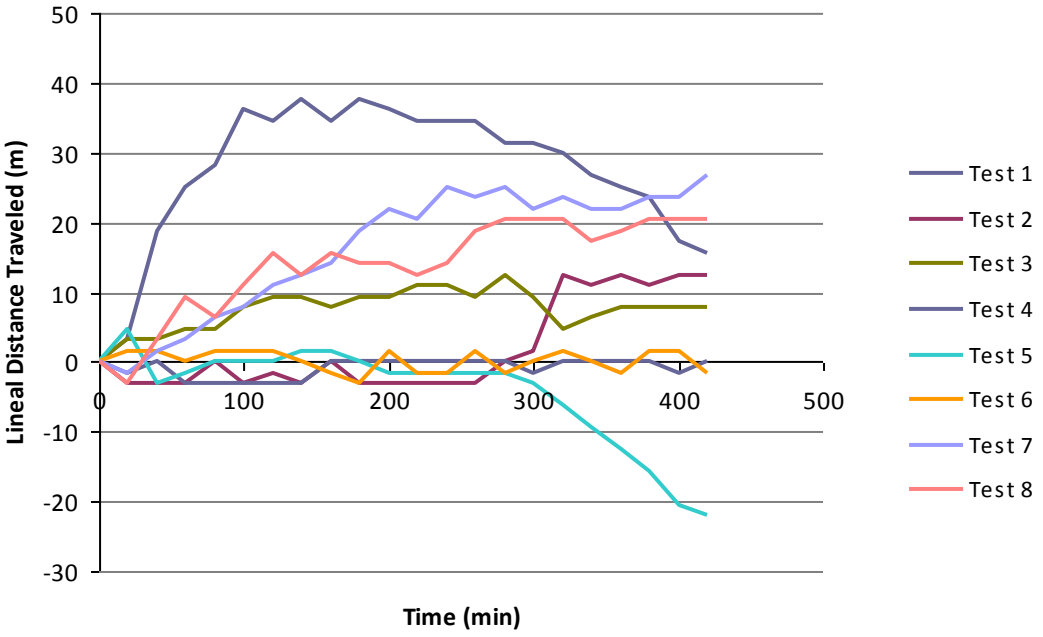

Figure 4-16. Position time-series for Mark II diffuser on tests

The position time-series for all trails are compiled, for the Mark II and III barrier tests, to generate the spatial variance of the carp at a specified time step of 20 mins. Each test represents the movements of one individual carp, apart from some population; therefore, the spatial variance is a result of dispersion as opposed to pure diffusion. The low carp population during the testing may cause the advective portion to dominate. Due to the limited number of trails, the variance for each time step was calculated from 7 or 8 data points for the diffuser on tests. As the control tests were assumed to be identical between trials, 15 data points are used to calculate the variance at each time step for the control tests. Figure 4-17 displays the spatial variance of the control tests for the Mark II and Mark III barrier tests combined.

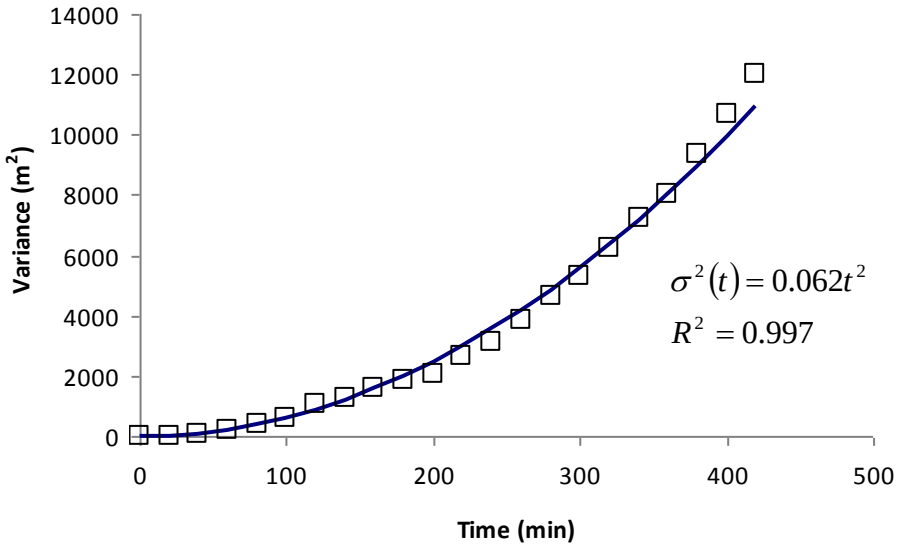

Figure 4-17. Dispersion of carp during control tests from Mark II and III trials combined

Note that the spatial variance of carp movement does not follow a linear trend, but a power-law trend. Following Metlzer et al. [2000], a system exhibiting anomalous transport, the variance is described by a power-law trend such as:

$$\sigma^2(t) = K_\alpha t^\alpha \qquad (4\text{-}1)$$

Where

α = diffusion exponent

K_α = diffusion coefficient

In equation (4-1) $0 < \alpha < 1$ signifies subdiffusive behavior, $1 < \alpha < 2$ signifies superdiffusive behavior, and $\alpha = 1$ is normal diffusion. Superdiffusive behavior, dispersal following a trend faster than that described by Brownian diffusion, indicated by the exponent value greater than 1 was expected based on the outlier carp in Figure 4-15. The close correlation of power trend line does indicate that carp movement without the barrier can be characterized by some random walk model, potentially a Lévy-flight

model. Figure 4-18 displays the dispersion of carp during the Mark II and Mark III diffuser on trials, separately.

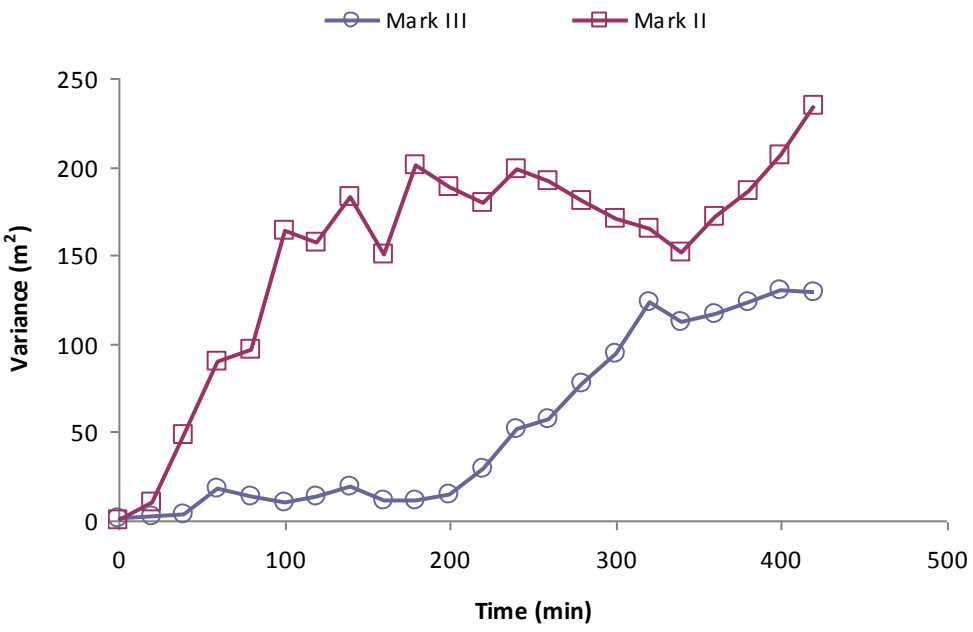

Figure 4-18. Dispersion of carp during Mark II and Mark III diffuser on trials

Note that the variance of the diffuser on trials results in no discernable trend; therefore, it can not be modeled by a random walk model. A breakdown of the spatial variance trend between the control and diffuser on tests indicates that a distinct behavioral change occurs. Change in carp behavior, whether it is from an avoidance response or just stress, indicates that the Mark II and Mark III barriers each provide a significant stimuli that carp detect and respond to.

Chapter 5.0 Discussion of Results

5.1 Physical Fields

A main goal of this research was to identify and quantify the physical fields that are generated by bubble curtains, and how they may be manipulated to improve bubble barrier designs. This research appears to be the first attempt to quantitatively measure the physical fields generated by bubble curtains in relationship to fish barrier technologies. The two main fields of focus are the hydrodynamic and acoustic. The experiments using the fine- and coarse-bubble diffusers indicate that the hydrodynamic field may be controlled by bubble size; however, it is important to highlight that the fine-bubble diffuser expressed bubbles across the entire surface of the diffuser while the coarse-bubble diffuser only expressed bubbles from one line of holes. The average velocities generated by the curtains do not exceed those expected in the interconnecting channels during high flow events; possibly decreasing the effect of the recirculation cell on deterring passage. The bubble size, formation rate, and depth of water did not greatly affect the size of the smallest eddies present in the flow, with the Kolmogorov length scale ranging from 0.04 to 0.08 mm for all trials. As the flow conditions generated by the bubble curtain do not appear to be drastically different that those occurring naturally, the hydrodynamic forces applied to the carp may not be the leading cause of avoidance.

The acoustic field generated by the bubble curtain appears to be the primary field that causes a behavioral change in the carp; as the maximum SPL varied greatly for each barrier design. The maximum SPL typically occurred around 150 Hz at a level between

90-130 dB. A range of 40 decibels is significant as the logarithmic unit equates to for every 20 decibels gained, the sound pressure (in kPa) increases ten-fold. A primary frequency at 150 Hz is much lower than the expected bubble resonant frequency calculated from equation 2-1; therefore, the maximum SPL created by each diffuser may be a result of bubble formation rate as opposed to the individual bubble physical characteristics. The data also clearly indicates that the larger bubbles generated a much greater SPL, which is expected from the relationship of equation 2-2. As the amplitude of bubble wall oscillations of a 5mm diameter bubble was 300 times greater than from 1mm diameter bubbles adds to the greater expected pressure via equation 2-2. The use of an ultra coarse-bubble diffuser for the Mark II and III barriers is a direct reflection of the relationship of bubble size to SPL strength.

Rapid attenuation is an important aspect of shallow water to consider in the design of an acoustic barrier operating within the carp's target sensitivity range of 100-500 Hz. Sound in this frequency range from any source will attenuate extremely fast, as Figure 2-18 illustrates, creating a natural acoustic gradient. The acoustic barriers tested by Taylor et al. [2005] and Welton et al. [2002] both featured underwater transducers as the main source of sound in the barriers and the bubble curtain is used to trap the sound, theoretically creating an even steeper gradient. Transducers provide reliable sound sources that, in preliminary tests, generate a maximum SPL exceeding 160 dB. Meaning that in 25 cm of water, a 160 dB sound source at 150 Hz will attenuate back to a background level of 80 dB in approximately 65 cm. The addition of bubbles to further

attenuate the sound does not seem likely, as Nehls et al. [2007] demonstrated that a bubble curtain attenuates a broadband noise approximately 5-10 dB. A similar loss would be expected in 5-10 cm distance away from the barrier, which happens to be the thickness of the bubble curtain itself. The use of bubbles to trap sound may be more effective at greater depths, where natural attenuation does not dominate at low frequencies. In shallow depths the bubble curtains paired with transducers may not increase the effectiveness of the barrier, assuming the acoustic field is the dominant deterrent. The increased SPL range of a transducer; however, may not be necessary in shallow conditions, as the Mark II barrier was able to generate a broad spectrum sound at approximately 80% of the signal strength of a transducer and resulted in a 75% reduction of passages.

5.2 Barrier Designs

The main hypothesis behind the design of the barriers used in this research was that the acoustic field generated by the bubble curtains was the primary deterrent of carp. This hypothesis was not fully tested as no behavioral tests were performed that isolated specific fields or sensory systems. However, this research did show that bubble barriers are capable of generating sound within the detection range of carp and that an avoidance response was clear. Whether the avoidance response was caused by acoustic stimuli or not cannot be confirmed at this time.

Each subsequent barrier increased either the intensity or breadth of the acoustic field in an attempt to see if carp behavior becomes altered. Figure 4-17 and 4-18 clearly indicate that the carp behavior was altered as a result of the barriers, and the effectiveness of the Mark II and Mark III barriers resulted in 75% reduction in passages in each direction. Tentatively, the results indicate that the bubble barrier has significant promise as an effective barrier technology in shallow, narrow channels. However, the effect of counter-current flow generated by the barrier may have created some biasing in the results. During the control tests, the water had an average velocity of 5 cm/s over the barrier; while no net flow was quantified over the barrier with air supplied as a result of recirculation cells on either side of the barrier. The data indicated that the carp continued making a similar number of passages between antennas with and without air supplied. The best option to eliminate the net flow reduction is to install a barrier in a linear stream where water must flux over the barrier due to gravity. Another possible means to increase the rigor of the testing procedure would be to attract fish through the use of food or some other attractant. The carp obviously had some motivation to move during the trials, as is seen in Figure 4-7 and 4-12. In reality, the carp will be driven by lack of food, escaping hypoxic conditions, or any number of other factors that would increase the carp's likelihood of crossing. The current trial serves as an initial phase of development and any basic reduction in passages was deemed a success; however, this shortcoming emphasizes the need for barrier testing in the field.

Chapter 6.0 Conclusions and Recommendations

The main objective of this research was to develop a bubble barrier design that could be used to deter carp in small streams, as well as characterize the physical fields generated by the bubble barrier. The following conclusions were reached through this research:

1. Bubble curtains generate distinct flow fields characterized by recirculation cells with an influence range of +/- 1-2 depths away from the diffuser in stagnant flow conditions.
2. A bubble curtain generates an acoustic field that has a peak SPL at 150 Hz (within the highest sensitivity range for carp) with a SPL magnitude between 90-130 dB. The acoustic signal is highly complex with significant frequency components within total carp hearing range.
3. The coarse-bubble diffusers generate stronger acoustic field than the fine-bubble diffuser; however, the fine-bubble diffuser generates a slightly stronger flow field than the coarse-bubble diffusers (17cm/s > 13cm/s).
4. The barrier trial results clearly demonstrates the accuracy and effectiveness of the RFID PIT tag detection system. The experimental configuration and testing protocal proved to be an effective method for the initial testing of the bubble barrier designs.
5. The Mark I barrier results indicate that a 10 second delay on the carp passage over the barrier is achieved; however, no significant stoppage was observed.
6. The Mark II and Mark III barriers resulted in a 75% average decrease in carp passages in the up- and down-stream directions.

7. Analysis of carp dispersion during control tests revealed a power-law relationship that may indicate carp dispersal is anamolous in nature.

Based on the results of the barrier tests, and the increasing magnitude of the maximum SPL between the barrier designs, the major barrier design hypothesis is that the acoustic field is the primary deterrent stimuli for bubble curtain barriers. The testing procedures for the current work did not allow for testing of specific stimuli input. The following is a collection of future work that would further development of bubble barrier technologies for common carp:

1. Quantify the effect of channel flow on the acoustic and hydrodynamic properties of a bubble curtain.
2. Perform more rigorous testing that includes, but not limited to, isolating either the hydrodynamic or acoustic fields of the barrier or sensory systems in the carp to identify the specific stimuli that causes the most significant change in carp behavior.
3. Using the similar testing procedures and apparatus, compare the barriers designed in this research with current technologies available commercially to identify any advantage or disadvantages to either design.
4. Field test a barrier design with existing carp populations in a specific field site or using laboratory carp populations, test the design using the SAFL Outdoor Stream Lab.

In summary, the bubble barrier designs considered in this research present a substantial promise as an effective carp barrier in shallow channels. The flexibility of the bubble curtain to adjust instantaneously with water depth and minimum decrease in field strength due to depth makes bubble curtains ideal for flashy streams. A 75% reduction in passages could provide a sizable decrease in the recruitment of juvenile carp from nursery lakes, consequently increasing the effectiveness of current carp management techniques in the main water bodies.

Chapter 7.0 References

Akamatsu, T., T. Okumura, N. Novarini, and H. Y. Yan. 2002. Empirical refinements applicable to the recording of fish sounds in small tanks. *The Journal of the Acoustical Society of America* 112 (6) (Dec): 3073-82.

Bajer, Przemyslaw, and Peter Sorensen. 2010. Recruitment and abundance of an invasive fish, the common carp, is driven by its propensity to invade and reproduce in basins that experience winter-time hypoxia in interconnected lakes. *Biological Invasions* 12 (5) (-05-01): 1101-12.

Bajer, Przemyslaw, Gary Sullivan, and Peter Sorensen. 2009. Effects of a rapidly increasing population of common carp on vegetative cover and waterfowl in a recently restored midwestern shallow lake. *Hydrobiologia* 632 (1) (-10-01): 235-45.

Brevik, I., and Ø. Kristiansen. 2002. The flow in and around air-bubble plumes. *International Journal of Multiphase Flow* 28 (4) (4): 617-34.

Brigham, E. Oran. 1974. *The fast fourier transform*. Englewood Cliffs, N.J.: Prentice-Hall.

Chen, Huey-Long, Miki Hondzo, and A. R. Rao. 2001. Estimation of turbulent kinetic energy dissipation. *Water Resources Research* 37 (6): 1761-9.

Dawson, H. A., U. G. Reinhardt, and J. F. Savino. 2006. Use of electric or bubble barrier to limit the movement of eurasion ruffe (*gymnocephalus cernuus*). *J. Great Lakes Res.*(32): 40-49.

EPRI. 1998. *Evaluation of fish behavioural barriers.* Palo Alto CA: TR-109483.

Fannelop, T. K., S. Hirschberg, and J. Küffer. 1991. Surface current and recirculating cells generated by bubble curtains and jets. *Journal of Fluid Mechanics* 229 (1): 629-57.

French, John, Douglas Wilcox, and S. Jerrine Nichols. 1999. Passing of northern pike and common carp through experimental barriers designed for use in wetland restoration. *Wetlands* 19 (4) (-12-01): 883-8.

Ghysen, Alain, and Christine Dambly-Chaudière. 2004. Development of the zebrafish lateral line. *Current Opinion in Neurobiology* 14 (1) (2): 67-73.

Hapca, Simona, John W. Crawford, Keith MacMillan, Mike J. Wilson, and Iain M. Young. 2007. Modelling nematode movement using time-fractional dynamics. *Journal of Theoretical Biology* 248 (1) (9/7): 212-24.

Kojima, Takahito, Hirosuke Ito, Tomoyuki Komada, Toru Taniuchi, and Tomonari Akamatsu. 2005. Measurements of auditory sensitivity in common carp cyprinus carpio

by the auditory brainstem response technique and cardiac conditioning method. *Fisheries Science* 71 (1) (02): 95-100.

Kundu, Pijush. 1990. *Fluid mechanics*. San Diego: Academic Press.

Leighton, T. G. 1994. *The acoustic bubble*. London ; San Diego: Academic Press.

Leighton, T. G., and A. J. Walton. 1987. An experimental study of the sound emitted from gas bubbles in a liquid. Abstract. *European Journal of Physics* 8, no. 2:98.

Lin, J. N., S. K. Banerji, and H. Yasuda. 1994. Role of interfacial tension in the formation and the detachment of air bubbles. *Langmuir* 10 (3) (03/01): 936-42.

Magnuson, John J., Annamarie L. Beckel, Ken Mills, and Stephen B. Brandt. 1985. Surviving winter hypoxia: Behavioral adaptations of fishes in a northern wisconsin winterkill lake. *Environmental Biology of Fishes* 14 (4) (-12-01): 241-50.

Meadows, B. S. 1973. Toxicity of rotenone to some species of coarse fish and invertebrates. *Journal of Fish Biology* 5 (2): 155-63.

Metzler, Ralf, and Joseph Klafter. 2000. The random walk's guide to anomalous diffusion: A fractional dynamics approach. *Physics Reports* 339 (1) (12): 1-77.

Nehls, G., K. Betke, S. Eckelmann, and M. Ros. 2007. *Assessment and costs of potential engineering solutions for the mitigation of the impacts of underwater noise arising from the construction of offshore windfarms.* COWRIE Ltd., COWRIE ENG-01-2007.

Patrick, Paul H., A. E. Christie, D. Sager, C. Hocutt, and J. Stauffer Jr. 1985. Responses of fish to a strobe light/ air-bubble barrier. *Fisheries Research* 3 : 157-72.

Popper, Arthur N. 1972. Pure-tone auditory thresholds for the carp, cyprinis carpio. *The Journal of the Acoustical Society of America* 52 (6) (12/00): 1714-7.

Popper, Arthur N., and Thomas J. Carlson. 1998. Application of sound and other stimuli to control fish behavior. *Transactions of the American Fisheries Society* 127 (5) (09/01): 673-707.

Ramirez, Robert W. 1985. *The FFT, fundamentals and concepts*. Englewood Cliffs, N.J.: Prentice-Hall.

Riess, I. R., and T. K. Fannelop. 1998. Recirculating flow generated by line-source bubble plumes. *Journal of Hydraulic Engineering* 124 (9) (09): 932.

Taft, E. P. 2000. Fish protection technologies: A status report. *Environmental Science & Policy* 3 (Supplement 1) (9/1): 349-59.

Taylor, R. M., M. A. Pegg, and J. H. Chick. 2005. Response of bighead carp to a bioacoustic behavioural fish guidance system. *Fisheries Management and Ecology*(12): 283-6.

Tonolla, Diego, Mark S. Lorang, Kurt Heutschi, and Klement Tockner. 2009. A flume experiment to examine underwater sound generation by flowing water. *Aquatic Sciences - Research Across Boundaries* 71 (4): 449.

Urick, Robert J. 1975. *Principles of underwater sound*. Rev ed. New York: McGraw-Hill.

Webb, Jacqueline F., Richard R. Fay, and Arthur N. Popper, eds. 2008. *Fish bioacoustics*. Springer handbook of auditory research. Vol. 32. New York, NY: Springer Science+Business Media, LLC.

Welton, J. S., R. C. Beaumont, and R. T. Clarke. 2002. The efficacy of air, sound and acoustic bubble screens in deflecting atlantic salmon *salmo salar L*., smolts in the river frome, UK. *Fisheries Management and Ecology*(9): 11-18.

Zhang, Xiaoxian, Scott N. Johnson, John W. Crawford, Peter J. Gregory, and Iain M. Young. 2007. A general random walk model for the leptokurtic distribution of organism movement: Theory and application. *Ecological Modelling* 200 (1-2) (1/10): 79-88.

Zydlewski, G. Barbin, A. Haro, and S. D. McCormick. 2005. Evidence for cumulative temperature as an initiating and terminating factor in downstream migratory behavior of atlantic salmon (salmo salar) smolts. *Canadian Journal of Fisheries and Aquatic Sciences* 62 (1): 11.

Appendix A. Results of Carp Behavioral Test Retest

Juvenile carp used in the behavioral tests of the Mark II and Mark III barriers were reused between tests. The tests were completed two months apart, with the goal of eliminating any experience possibly gained by fish subjected to the barrier-on trials. To confirm that carp would exhibit no changed behavior around the barrier, a small group of experienced carp was retested only one month after Mark II tests concluded. The retest consisted of three groups of three fish (3 PIT tagged, 6 untagged). The fish used for retesting were randomly selected out of the whole population to remove any biasing. The retest consisted of placing each group in the test tank with the Mark II barrier on. If any previous experience with the barrier negatively impacts future results, the number of passages should reflect an increase in passages in comparison to the Mark II test results. If passages remained low, future barrier tests would not be affected by previous experience, after waiting one month between uses of the fish. The previous experience of the PIT tagged fish in each group was identified to make sure at least one barrier-on and one control fish was retested. The following table provides the total number of passages performed by each group of fish in the up- and down-stream directions. Note that the previous experience of the PIT tagged fish is listed in the last column.

Results of Behavioral Retest

Test #	Upstream Passages	Downstream Passages	Previous Experience
1	0	0	Barrier-On
2	0	0	Barrier-On
3	40	33	Control

The results of the first two retests indicate that barrier experience did not reduce the effectiveness of the barriers. Test 3 had clearly showed an increase in passages; however these values were within or just outside the expected range for previously virgin carp exposed to the Mark II barrier-on trials. The average number of passage attempts in each direction with standard deviations for the Mark II barrier-on tests were 16±14 (upstream) and 20±18 (downstream).